

מכון ויצמן למדע

WEIZMANN INSTITUTE OF SCIENCE



## Variants in PUS7 Cause Intellectual Disability with Speech Delay, Microcephaly, Short Stature, and Aggressive Behavior

### Document Version:

Accepted author manuscript (peer-reviewed)

### Citation for published version:

De Brouwer, APM, Abou Jamra, R, Koertel, N, Soyris, C, Polla, DL, Safra, M, Zisso, A, Powell, CA, Rebelo-Guioamar, P, Dinges, N, Morin, V, Stock, M, Hussain, M, Shahzad, M, Riazuddin, S, Ahmed, ZM, Pfundt, R, Schwarz, F, de Boer, L, Reis, A, Grozeva, D, Raymond, FL, Riazuddin, S, Koolen, DA, Minczuk, M, Roignant, J-Y, van Bokhoven, H & Schwartz, S 2018, 'Variants in PUS7 Cause Intellectual Disability with Speech Delay, Microcephaly, Short Stature, and Aggressive Behavior', *American Journal of Human Genetics*, vol. 103, no. 6, pp. 1045-1052. <https://doi.org/10.1016/j.ajhg.2018.10.026>

Total number of authors:

28

### Digital Object Identifier (DOI):

[10.1016/j.ajhg.2018.10.026](https://doi.org/10.1016/j.ajhg.2018.10.026)

### Published In:

American Journal of Human Genetics

### License:

CC BY-NC-ND

### General rights

@ 2020 This manuscript version is made available under the above license via The Weizmann Institute of Science Open Access Collection is retained by the author(s) and / or other copyright owners and it is a condition of accessing these publications that users recognize and abide by the legal requirements associated with these rights.

### How does open access to this work benefit you?

Let us know @ [library@weizmann.ac.il](mailto:library@weizmann.ac.il)

### Take down policy

The Weizmann Institute of Science has made every reasonable effort to ensure that Weizmann Institute of Science content complies with copyright restrictions. If you believe that the public display of this file breaches copyright please contact [library@weizmann.ac.il](mailto:library@weizmann.ac.il) providing details, and we will remove access to the work immediately and investigate your claim.

**Variants in *PUS7* cause intellectual disability with speech delay, microcephaly, short stature, and aggressive behavior.**

Running title: *PUS7* variants cause neurodevelopmental and growth delay.

Arjan PM de Brouwer<sup>1,\*</sup>, Rami Abou Jamra<sup>2,3,\*</sup>, Nadine Körtel<sup>4,\*</sup>, Clara Soyris<sup>5</sup>, Daniel L Polla<sup>1,6</sup>, Modi Safra<sup>5</sup>, Avia Zisso<sup>5</sup>, Christopher A Powell<sup>7</sup>, Pedro Rebelo-Guiomar<sup>7</sup>, Nadja Dinges<sup>4</sup>, Violeta Morin<sup>4</sup>, Michael Stock<sup>4</sup>, Mureed Hussain<sup>1,8,9</sup>, Mohsin Shahzad<sup>10</sup>, Saima Riazuddin<sup>9</sup>, Zubair M. Ahmed<sup>9</sup>, Rolph Pfundt<sup>1</sup>, Franziska Schwarz<sup>1</sup>, Lonneke de Boer<sup>11</sup>, André Reis<sup>2</sup>, Detilina Grozeva<sup>12</sup>, F Lucy Raymond<sup>12</sup>, Sheikh Riazuddin<sup>8,10,13</sup>, David A. Koolen<sup>1</sup>, Michal Minczuk<sup>7</sup>, Jean-Yves Roignant<sup>4#</sup>, Hans van Bokhoven<sup>1#</sup>, Schraga Schwartz<sup>5#</sup>

1. Department of Human Genetics, Donders Institute for Brain, Cognition and Behaviour, Radboud university medical center, 6500HB, Nijmegen, The Netherlands.
2. Institute of Human Genetics, Friedrich-Alexander-Universität Erlangen-Nürnberg, 91054 Erlangen, Germany.
3. Institute of Human Genetics, University Medical Center Leipzig, 04109 Leipzig, Germany.
4. Laboratory of RNA Epigenetics, Institute of Molecular Biology (IMB), 55128 Mainz, Germany.
5. Department of Molecular Genetics, Weizmann Institute of Science, Rehovot 76100, Israel
6. CAPES Foundation, Ministry of Education of Brazil, 70040-020, Brasília, Brazil.
7. CAP, PR-G, MM: MRC Mitochondrial Biology Unit, University of Cambridge, Cambridge, CB2 0XY, UK.
8. National Centre of Excellence in Molecular Biology, University of The Punjab, Lahore 53700, Pakistan.
9. Department of Otorhinolaryngology—Head and Neck Surgery, University of Maryland, School of Medicine, Baltimore, MD 21201-1734, USA.

10. Center for Genetic Diseases, Shaheed Zulfiqar Ali Bhutto Medical University, Pakistan  
Institute of Medical Sciences, Islamabad 44000, Pakistan.
11. Department of Paediatrics, Radboud Center for Mitochondrial Medicine, Radboudumc,  
6525 GA, Nijmegen, The Netherlands.
12. Department of Medical Genetics, University of Cambridge, Cambridge, CB2 0QQ, United  
Kingdom.
13. Allama Iqbal Medical College, University of Health Sciences, Lahore 54600, Pakistan.

\* These first authors contributed equally to the manuscript

# These senior authors contributed equally to the manuscript

Correspondence to: Schraga Schwartz, PhD  
Department of Molecular Genetics  
Weizmann Institute of Science, Rehovot, Israel  
Email: [schwartz@weizmann.ac.il](mailto:schwartz@weizmann.ac.il)

Correspondence to: Arjan de Brouwer, PhD  
Department of Human Genetics 855  
Radboud University Nijmegen Medical Centre  
P.O. Box 9101, 6500 HB Nijmegen, The Netherlands  
E-mail: [Arjan.deBrouwer@radboudumc.nl](mailto:Arjan.deBrouwer@radboudumc.nl)  
Tel: 0031 (0)24 3617431  
Fax: 0031 (0)24 3668753

Abstract word count: 129 (max 250)

Manuscript word count: 2734 (max 3600)

Number of references: 38

Number of figures: 3

Number of tables: 1

Online supplemental data: 7 figures, 3 tables, detailed clinical descriptions, and methods

## Abstract

We describe six persons from three families with three homozygous protein truncating variants in *PUS7*: c.89\_90del, p.(Thr30Lysfs\*20); c.1348C>T, p.(Arg450\*); and a deletion of the penultimate exon 15. All these individuals have intellectual disability with speech delay, short stature, microcephaly, and aggressive behavior. *PUS7* encodes the RNA-independent pseudouridylate synthase 7. Pseudouridylation is the most abundant post-transcriptional modification in RNA, which is primarily thought to stabilize secondary structures of RNA. We show that the disease-related variants lead to abolishment of *PUS7* activity on both tRNA and mRNA substrates. Moreover, *Pus7* knockout in *Drosophila melanogaster* results in a number of behavioral defects, including increased activity, disorientation, and aggressiveness supporting that neurological defects are caused by *PUS7* variants. Our findings demonstrate that RNA pseudouridylation by *PUS7* is essential for proper neuronal development and function.

## Main text

Pseudouridylation is the most abundant post-transcriptional modification of RNA.<sup>1; 2</sup> Pseudouridine (5-ribosyluracil,  $\Psi$ ) is the 5-ribosyl isomer of uridine.<sup>1</sup> It was the first modified nucleoside to be discovered in RNA and is found in transfer RNA (tRNA),<sup>3; 4</sup> small nuclear RNA (snRNA),<sup>5</sup> small nucleolar RNA (snoRNA),<sup>1</sup> ribosomal RNA (rRNA),<sup>6; 7</sup> and more recently also in messenger RNA (mRNA).<sup>8-11</sup> RNA pseudouridylation can lead to a stabilization of the 3D structure of RNA<sup>12; 13</sup> by an altered RNA structure,<sup>14</sup> increased base stacking,<sup>15</sup> improved base-pairing<sup>16</sup> and a rigidified sugar-phosphate backbone.<sup>17</sup> Pseudouridylation in human is catalyzed by 13 pseudouridine synthases (PUSs), which are either guided to their targets via small nucleolar RNAs (snoRNAs), or directly recognize their targets in an RNA-independent manner.<sup>1; 18</sup>

Variants in genes that code for RNA-independent pseudouridine synthases have been shown to result in a monogenic disorder. Recessively inherited *PUS1* [MIM: 608109] pathogenic variants cause defective oxidative phosphorylation resulting in progressive mitochondrial myopathy and sideroblastic anemia (MLASA syndrome [MIM: 600462]).<sup>19</sup> In addition, growth delay, secondary microcephaly, and intellectual disability have been reported in multiple individuals.<sup>20-24</sup> Recently, a second pseudouridylation defect has been described in a single consanguineous family with a homozygous *PUS3* [MIM: 616283] variant, another RNA independent pseudouridine synthase.<sup>25</sup> Affected family members have severe to profound intellectual disability, microcephaly, and severe growth deficiency. Both pseudouridine synthases modify tRNA at various positions, suggesting that reduced pseudouridylation of tRNA may cause progressive monogenic multisystemic diseases centered around a general failure to thrive and neurodevelopmental delay.

*PUS7* [MIM: 616261] encodes RNA-independent pseudouridylate synthase 7. Both yeast and human *PUS7* recognize a UG $\Psi$ AG core motif.<sup>8; 26</sup> Yeast *PUS7* modifies U2 snRNA at position 35,<sup>5; 8</sup> several tRNAs at position 13, position 35 in pre-tRNA(Tyr),<sup>27</sup> and a large number of mRNAs, the latter in particular upon a heat shock.<sup>8</sup> Human *PUS7* was shown to modify tRNAs and tRNA-derived small fragments (tRFs).<sup>28</sup> Pseudouridylation of tRFs is

required for early embryogenesis and for hematopoiesis. In addition, human PUS7 targets dozens to hundreds of different mRNAs implicated in a range of functions.<sup>8; 11; 26</sup> Here, we describe six persons from three independent families with deleterious biallelic variants in *PUS7* resulting in neurodevelopmental and growth delay. Written informed consent was obtained for all individuals involved. This study adhered to the World Health Association Declaration of Helsinki (2013) and was approved by the Institutional Review Board (IRB) of the Centre of Excellence in Molecular Biology (CEMB), University of the Punjab, Lahore, Pakistan, by the ethic committee at the University of Nüremberg-Erlangen in Germany, and the institutional review board Commissie Mensgebonden Onderzoek Regio Arnhem-Nijmegen.

Family 1 (PKMR215; **Fig. 1A; Table 1**) originates from Pakistan and has been described briefly before by Riazuddin *et al.* (2016)<sup>29</sup> as a family with moderate ID, speech delay and aggressive behavior (see **Supplemental Note**). The parents of the four affected siblings (IV2-5) are first cousins. The three affected individuals who are still alive (aged 7-18 years), presented with moderate intellectual disability, speech delay, and aggressive behavior. The two oldest siblings (IV-2 and IV-3) who were approachable for further evaluation also had short stature, low weight, and microcephaly. Pregnancy and delivery were uneventful and birth parameters within normal range for all affected family members.

Family 2 (MR046; **Fig. 1B; Table 1**) stems from the Southern part of Syria. The parents are first degree cousins. They have two sons (IV-1 and IV-2) with a moderate intellectual disability, motor and speech delay (see **Supplemental Note**). The oldest sibling (IV-1) of 8 years-old showed hyperactive, aggressive, and destructive behavior. Both siblings had short stature, and microcephaly. Weight was not determined at the time of investigation, but their BMI was visibly in the lower normal range. Pregnancies of both children were uneventful. However, the parents reported that at birth the elder boy had a small head, and that he seemed to be lifeless for the first 30 minutes after birth. The family is now lost for further follow-up.

Family 3 (R14-22173) is a consanguineous Dutch family of Moroccan descent in which one boy (II-2) has intellectual disability (**Fig. 1C; Table 1**). At the age of three months, he

presented with hypotonia and motor delay (see **Supplemental Note**). At the age of three years, he also presented with speech delay and aggressive behavior. His growth parameters were delayed as well as he had short stature, low weight, and microcephaly. Pregnancy and delivery were uneventful, however the neonatal period was complicated by feeding difficulties and hypopnea, requiring tube feeding and respiratory support for three weeks.

Exome sequencing was performed on DNA from one (Family 2 and 3) or two (Family 1) affected individuals from each of the three families. In family 1, a homozygous c.89\_90del frameshift variant (p.(Thr30Lysfs\*20)) was identified in *PUS7* (GenBank: NM\_019042.3;**Fig. S1A**). Sanger sequencing showed that this variant was homozygously present in the affected siblings, heterozygously in the parents, and absent in the unaffected sibling (**Fig. S1B**). This variant is predicted to result in nonsense-mediated mRNA decay. Accordingly, quantitative PCR (qPCR) analysis showed that *PUS7* mRNA levels in Epstein Barr-Virus-transformed lymphoblastoid cell lines (EBV-LCLs) from family member IV-3 were 1.8-fold ( $P=0.036$ ) reduced as compared to those in EBV-LCLs from healthy control individuals (**Fig. S2A**). Western blot analysis confirmed the absence of a normally sized *PUS7* protein in this affected individual (**Fig. S2B**).

In family 2, we performed homozygosity mapping<sup>30</sup> with the use of HomozygosityMapper<sup>31</sup>. After sequencing the index and evaluating the data as previously described<sup>32</sup>, a homozygous c.1348C>T nonsense variant (p.(Arg450\*)) was identified in *PUS7* (**Fig. S1A**). Both affected brothers carried this variant homozygously and the mother was a heterozygous carrier (**Fig. S1C**). Their father was not available for testing. This variant is also predicted to result in nonsense-mediated mRNA decay and qPCR analysis established that *PUS7* mRNA levels in family member IV-1 were indeed 15.6-fold ( $P<0.0001$ ) reduced as compared to those in controls (**Fig. S2A**).

In family 3, exome sequencing was performed on both the affected male individual and his parents. No potentially causative *de novo*, biallelic, or X-linked single nucleotide variants or indels were found. CNV analysis of the exome data of the affected individual indicated a potential deletion of the last two exons of *PUS7*, which had not been identified by



the earlier-performed chromosomal microarray analysis, likely because of the small size of the deletion (max. 5kb). Multiplex amplification quantification analysis confirmed a homozygous deletion of only exon 15 in the affected individual (**Fig. S1D**). This deletion was heterozygously present in his father and absent in DNA from his brother. Genetic testing could not be performed in the mother. Reverse transcriptase PCR analysis confirmed that exon 15 was indeed absent from *PUS7* mRNA (**Fig. S1E**). The penultimate exon 15 of *PUS7* comprises 92 bp. A deletion of this exon results in a frameshift removing the C-terminus of PUS7 including 56 amino acid residues of the TruD catalytic domain (**Fig. S1A**). Since the resulting premature stop codon is positioned after the last exon-exon boundary, *PUS7* mRNA from affected individuals is likely to escape nonsense-mediated RNA decay. Accordingly, *PUS7* mRNA levels in EBV-LCLs from family member II-2 were normal (**Fig. S2A**). In addition, Western blot analysis confirmed the absence of a normally sized PUS7 protein in this affected individual (**Fig. S2B**).

The phenotype of our six persons with a pathogenic *PUS7* variant closely resembles that of the single family with a homozygous *PUS3* variant (MRT55 [MIM: 617051]).<sup>25</sup> The three affected family members with a *PUS3* variant also presented with intellectual disability, secondary microcephaly, and short stature. Additionally, coarse facial features, strabismus, gray sclera and extensive Mongolian spots were noted, which were not present in our affected individuals. Remarkably, persons with recessively inherited *PUS1* variants have intellectual disability, microcephaly, and growth delay as well.<sup>20-24</sup> This indicates that these three syndromes are closely related and can be defined by neurodevelopmental and growth delay. *PUS1*, *PUS3*, and *PUS7* are expressed in all tissues analyzed (**Fig. S3**). The milder phenotype in affected family members with deleterious *PUS7* variants might be related to the lower overall average *PUS7* expression levels as compared to *PUS1* and *PUS3*. The relatively high *PUS7* expression levels in cerebellum and tibial nerve support a more specific role for PUS7 in neurodevelopment.

In order to assess whether PUS7 activity on tRNAs was impacted in the affected individuals, we first performed radioactive primer extension experiments in the presence of

carbodiimide (CMC) followed by alkali treatment using total RNA from EBV-LCLs of individual IV-3 from family 1, primary fibroblasts individual II-2 from family 3, and corresponding controls (**Fig 2A; Fig S4**). This method relies on the ability of a CMC to form a covalent adduct with pseudouridine and to cause cDNA truncations upon reverse transcription, which can be quantified by primer extension. We detected a clear reduction in signal at  $\Psi$ 13 in tRNAGlu in material from affected individuals as compared to controls. In order to more systematically investigate the activity of PUS7, we also performed unbiased pseudouridylation mapping using  $\Psi$ -seq. This method also relies on reverse transcription truncations induced by CMC, but is followed by sequencing all of the truncation sites in RNA. This enables detection of the positions at which reverse transcriptase selectively dropped off upon treatment with CMC, compared to an untreated control.<sup>8</sup> We first applied  $\Psi$ -seq to total RNA extracted from four EBV-LCLs originating from controls, and two from affected individuals. Based on analysis of termination sites in CMC-treated samples in comparison to input, we assembled a dataset of 234 sites with consistent evidence of pseudouridylation across at least two of the samples, 161 of which (69%) originated from within tRNA molecules. We then performed a directed search for sites that underwent differential pseudouridylation between affected individuals and controls. Using strict criteria (both t-test  $p$ -value<0.05 and Chi-squared  $p$ -value<0.05), ten sites passed the threshold (**Table S1**). Strikingly, all of these sites were at position 13 of various tRNAs, a position orthologous to the known Pus7 modification site in budding yeast. To expand this analysis, we classified the 161 sites detected in tRNAs into families on the basis of the position within the tRNA that was modified and the pseudouridine synthases putatively catalyzing their formation. The major families represented in our dataset included position 13 ( $n=17$ ; putative PUS7 target), positions 27/28 ( $n=38$ ; in yeast substrates of PUS1<sup>33</sup>) and positions 38/39 ( $n=36$ ; substrates of PUS3<sup>34</sup>). This analysis revealed that the pseudouridylation signal in EBV-LCLs of affected individuals was essentially abolished at the PUS7 substrates at position 13, but not at the remaining positions (**Fig. 2B**). This confirms the specific abolishment of pseudouridine from position 13 of tRNAs within the two affected individuals harboring a variation in *PUS7*. To

expand this analysis, we also conducted  $\Psi$ -seq on total RNA from primary fibroblasts of individual II-2 from family 3 including corresponding controls, and observed a significant reduction of signal from position 13 of tRNAs ( $p$ -value $<0.05$ ; **Fig. S5**).

Position 35 in yeast U2 snRNA was previously shown to undergo pseudouridylation via Pus7.<sup>5; 8</sup> We thus assessed whether pseudouridylation at its mammalian counterpart, in human at position 34 of U2 snRNA, was impacted in the affected individuals. However, we did not observe decreased pseudouridylation at this position (**Fig. 2B**), most likely indicating that in human this modification is catalyzed via a different pseudouridine synthase. This is consistent with previous observations in *Xenopus* oocytes indicating that the pseudouridylation of this site is mediated by an H/ACA box small containing RNA.<sup>35</sup> In yeast, Pus7 also modifies position 35 in pre-tRNA(Tyr).<sup>27</sup> This position was insufficiently covered in our data, likely due to additional modifications on tRNA-Tyr that prevented efficient reverse transcription.

PUS7 has also been implicated in mRNA pseudouridylation. Therefore, we applied  $\Psi$ -seq to poly(A) enriched RNA derived from one affected individual and one control sample. We then quantified pseudouridylation signals across a pre-defined high-confidence catalog of PUS7 sites in mRNA, as well as across TRUB1 targets serving as controls.<sup>26</sup> This catalog was filtered to retain only sites for which we had sufficient coverage in the experiments and which showed minimal evidence for pseudouridylation in our samples. We observed a decrease in pseudouridylation levels across these nine PUS7 targets in affected individuals compared to controls (paired t-test,  $p=0.003$ ,  $n=9$ ) whereas no changes were observed in TRUB1 targets (paired t-test,  $p=0.43$ ,  $n=24$ ) (**Fig. 2D,E;Table S2**). Thus, PUS7 activity is strongly reduced and likely eliminated within mRNA targets in affected individuals.

*PUS7* variants identified in the three families thus result in aberrant pseudouridylation of at least ten cytosolic tRNAs at position 13. tRNAs are the main target of PUS7 as more than 70% of all PUS7-modified RNAs are tRNAs.<sup>28</sup> Both PUS1 and PUS3 also modify predominantly cytosolic tRNA at various positions, suggesting that aberrant tRNA pseudouridylation could be the common cause underlying neurodevelopmental and growth

delay. The more severe phenotype of persons with *PUS1* pathogenic variants consisting of MLASA syndrome<sup>19</sup> may be due to a dual role of PUS1 in modifying both cytosolic and mitochondrial tRNAs, in contrast to PUS7, which does not modify mitochondrial tRNAs. It is yet unknown whether PUS3 may pseudouridylate mitochondrial tRNAs. The pathogenicity of the *PUS7* variants may also be partially mediated by the dysregulated mRNA pseudouridylation profile, but the functional relevance of pseudouridine on mRNA remains to be established.

Next, we knocked out the uncharacterized *Pus7* homolog (CG6745) in *Drosophila melanogaster* to address whether PUS7 function is conserved across evolution. CG6745 is highly conserved between *Drosophila* and human with a DIOPT (Drosophila RNAi Screening Center Integrative Ortholog Prediction Tool) score of 12, which means 12 out of the 15 tools to identify orthologs indicate that CG6745 is the human ortholog of *PUS7*.<sup>36</sup> Using the CRISPR/Cas9 approach, we generated a small deletion of 13 nucleotides in the first half of the gene, which leads to an early frameshift and a premature stop codon (**Fig. 3A**). The resulting protein is expected to lack the entire Pus synthase domain.

As *Pus7* mutant flies were viable, we proceeded by evaluating the effect of the variant on fly behavior by applying the Buridan's paradigm<sup>37</sup>. We found that the overall activity of *Pus7* mutant flies was significantly increased (t-test analysis of variance with Bonferroni correction,  $p < 0.001$ ; **Fig. 3B**). In addition, severe orientation defects were observed as evidenced by a significantly larger angular deviation (t-test analysis of variance with Bonferroni correction,  $p < 0.01$ ) of their 15-minute walking traces (**Fig. 3C, 3D**). We obtained similar results when *Pus7* mutants were crossed with a deficiency line deleting the *Pus7* locus along with additional flanking genes, ruling out off-target effects. The increased activity of *Pus7* mutant flies may indicate that hyperactive behavior of affected individual IV-1 from family 2 may be directly related to the PUS7 variants. As individuals with a *PUS7* variant also exhibit aggressive behavior, we wondered whether this trait might be conserved in *Drosophila*. To address this possibility, we performed an aggression assay as described previously.<sup>38</sup> Briefly, single control and mutant adult males were placed in a small chamber

containing food at its center. The two flies compete for the food and exhibit several fighting behaviors that can be quantified (**Fig. S6**). Overall, we found that *Pus7* flies spent significantly more time fighting (**Fig. 3E**) and were most often the winner of the fight (**Fig. 3F**), indicating that they are more aggressive than their wild-type counterpart.

We next attempted to rescue the behavior defects by expressing *Pus7* cDNA in the *Pus7* mutant background. However, this experiment was inconclusive as overexpression of *Pus7* in wild-type context already strongly alters fly activity and orientation (**Fig. S7**). Notably, expression of *Pus7* only in neurons by using the *Elav-GAL4* driver was sufficient to alter fly behavior, suggesting that *Pus7* exerts its activity through a neuronal function. Altogether these findings demonstrate that *Pus7* controls several aspects of fly behavior and that its dosage must be tightly regulated.

Lastly, we performed  $\Psi$ -seq analysis on total RNA derived either from wild-type or *Pus7* mutant fly heads, and performed an unbiased search towards pseudouridylation sites deficient in the latter. Of 11 sites passing our thresholds, nine occurred at position 13 of diverse tRNAs (**Table S3**), indicating that the molecular role of *Pus7* is conserved between human and *Drosophila*.

In conclusion, we describe a syndrome consisting of intellectual disability, speech delay, microcephaly, short stature, and aggressive behavior, which is caused by deleterious *PUS7* variants. We demonstrate that the variants lead to a loss of *PUS7* activity on both tRNA and mRNA substrates. A role for *PUS7* in neurodevelopment is further corroborated by its relatively high expression levels in the brain and by *Pus7* knockout *Drosophila* that display hyperactivity, disorientation, and aggressiveness, likely due to a defective nervous system. Our findings strengthen the notion that RNA pseudouridylation and especially tRNA modification is essential for proper neuronal development.

## **Declaration of interest**

The authors declare no competing interests.

## **Acknowledgements**

We are very grateful to the families for their participation. We would like to thank Saskia van de Velde-Visser (Radboudumc, Nijmegen, the Netherlands) for technical assistance culturing the cell lines. We would like to thank Farah Radwan (Institute of Human Genetics, Erlangen, Germany) for technical assistance with genetic analysis of family 2. In addition, we thank the group of Prof. Roland Strauss, in particular Teuta Wille, for assistance with performing the Buridan paradigm experiments. This work was supported by the Action Medical Research and NIHR Biomedical Research Centre, UK [to FLR], the Israel Science Foundation (543165) and the European Research Council (ERC) under the European Union's Horizon 2020 research and innovation programme (grant agreement No. 714023), The Abramson Family Center for Young Scientists, the David and Fela Shapell Family Foundation INCPM Fund for Preclinical Studies, the Estate of David Turner, and the Berlin Family Foundation New Scientist Fund [to SS], by the DFG (Deutsche Forschungsgemeinschaft) AB393/2-2 [to RJ and AR] and RO4681/9-1 to [JYR], by the DIP RO4681/6-1 to [JYR], by CAPES Fellowship 99999.013311/2013-01 [to DLP], and by the EU FP7 Large-Scale Integrating Project Genetic and Epigenetic Networks in Cognitive Dysfunction (241995) [to HvB and SR], Higher Education Commission in Pakistan, the University of Maryland, and the Medical Research Council, UK (MC\_UU\_00015/4) [to CAP, PR-G and MM]. The funders had no role in design, conduct, analysis, and reporting of this study.

## Figure legends

**Figure 1.** Family pedigrees and photographs of affected individuals with a *PUS7* variant. **A)** Family 1 with the p.(Thr30Lysfs\*20) variant: IV-2 at the age of 18 and IV-3 at the age of 14 years. **B)** Family 2 with the p.(Arg450\*) variant: IV-1 at the age of 8 years and IV-2 at the age of 2 years. **C)** Family 3 with the exon 15 deletion: II-2 at the age of 3 years. Presence of the variant is indicated under the symbols in the pedigrees. - = reference allele; m = variant allele.

**Figure 2.** Persons with a *PUS7* variant are defective in tRNA and mRNA pseudouridylation. **A)** Primer extension analysis against human cytoplasmic tRNA-Glu applied to total RNA extracted from lymphoblasts (IV:3 and corresponding controls) and fibroblasts (II:2 and corresponding controls). **B)** Measurements of  $\Psi$  levels approximated via the  $\Psi$ -ratio across three classes of positions on tRNAs across four control samples, including heterozygous individual III:2 from family 2 (4603), and two samples from individual IV-1 from family 2 (4601) and individual IV:3 from family 1 (HEP1500058). ANOVA based p-values are presented. The depicted boxplots present the median (thick central line), first and third quartiles (bottom and top boundary of the box), 1.5\*the interquartile range (depicted by the whiskers), and outliers (presented as individual points). **C)**  $\Psi$ -ratios at position 34 of human snRNAs in non-treated samples (left panel) and upon CMC-treatment. **D)**  $\Psi$ -ratios within mRNAs, at either previously characterized targets of TRUB1 (left panel) or of PUS7 (right panel). Distributions are presented as boxplots, as in panel A. **E)** Graphical depiction of  $\Psi$ -ratios in regions surrounding PUS7 targets in a lncRNA and an mRNA. The position highlighted in yellow indicates the PUS7-mediated  $\Psi$  site. Stops in the control, but not in individual IV:3 from family 1, are present 1 bp downstream of this indicated position.

**Figure 3.** Behavioral defects in *Pus7* mutant *Drosophila*. **A)** Schematic representation of the Pus7 protein showing the conserved Pus synthase domain. The position of the frameshift

variant caused by the guide RNA-induced deletion is indicated in the schematic representation, the protein coding DNA sequence, and the protein itself. **(B-C)** Walking behavior of *Pus7* mutant flies in Buridan's paradigm. **B)** Activity; **C)** Median angular displacements from the direct approach to one of the stripes. Thirty flies (15 males and 15 females) were tested per genotype. NS, not significant; \*  $P < 0.05$ , \*\* $P < 0.01$ , \*\*\* $P < 0.001$  (t-test analysis of variance with Bonferroni correction). **D)** Representative examples of fly movement for each genotype. Red lines indicate when flies walked from one end to another. Blue lines indicate when flies did not walk the whole way but stopped and changed the direction back to the end where they started. **E)** Time spent fighting by the wild-type and *Pus7* mutant adult males and the winner of the fights are indicated. **F)** Winner of the fights between wild-type and *Pus7* mutant adult males. In total, ten pairs of flies were used for the quantification in E and F.



**Web Resources**

Online Mendelian Inheritance in Man (OMIM): <http://www.omim.org>

Genotype-Tissue Expression (GTEx) project: <https://gtexportal.org>

Gene Expression Omnibus (GEO): <https://www.ncbi.nlm.nih.gov/geo/>

## References

1. Charette, M., and Gray, M.W. (2000). Pseudouridine in RNA : What, Where, How, and Why. *IUBMB Life* 49, 341-351.
2. Zebarjadian, Y., King, T., Fournier, M.J., Clarke, L., and Carbon, J. (1999). Point mutations in yeast CBF5 can abolish in vivo pseudouridylation of rRNA. *Molecular and cellular biology* 19, 7461-7472.
3. Grosjean, H., Sprinzl, M., and Steinberg, S. (1995). Posttranscriptionally modified nucleosides in transfer RNA: Their locations and frequencies. *Biochimie* 77, 139-141.
4. Sprinzl, M., and Gauss, D.H. (1982). Compilation of sequences of tRNA genes. *Nucleic Acids Research* 10, 762-762.
5. Yu, A.T., Ge, J., and Yu, Y.T. (2011). Pseudouridines in spliceosomal snRNAs. *Protein and Cell* 2, 712-725.
6. Branlant, C., Krol, A., Machatt, M.A., Pouyet, J., and Ebel, J.-P. (1981). Primary and secondary structures of Escheria coli MRE 600 23S ribosomal RNA. Comparison with models of secondary structure for maize chloroplast 23S rRNA and for large portions of mouse and human 16S mitochondrial rRNAs. *Nucleic Acids Research* 9, 6953-6958.
7. Schattner, P., Barberan-Soler, S., and Lowe, T.M. (2006). A computational screen for mammalian pseudouridylation guide H/ACA RNAs. *RNA (New York, NY)* 12, 15-25.
8. Schwartz, S., Bernstein, D.A., Mumbach, M.R., Jovanovic, M., Herbst, R.H., Engreitz, J.M., Guttman, M., Satija, R., Lander, E.S., Fink, G., et al. (2014). Transcriptome-wide Mapping Reveals Widespread Dynamic-Regulated Pseudouridylation of ncRNA and mRNA. *Cell* 159,148-162.
9. Carlile, T.M., Rojas-Duran, M.F., Zinshteyn, B., Shin, H., Bartoli, K.M., and Gilbert, W.V. (2014). Pseudouridine profiling reveals regulated mRNA pseudouridylation in yeast and human cells. *Nature* 515, 143-146.
10. Lovejoy, A.F., Riordan, D.P., and Brown, P.O. (2014). Transcriptome-wide Mapping of Pseudouridines: Pseudouridine Synthases Modify Specific mRNAs in *S. cerevisiae*. *PLoS One* 9, e110799.
11. Li, X., Zhu, P., Ma, S., Song, J., Bai, J., Sun, F., and Yi, C. (2015). Chemical pulldown reveals dynamic pseudouridylation of the mammalian transcriptome. *Nat Chem Biol* 11, 592-597.
12. Leppik, M., Peil, L., Kipper, K., Liiv, A., and Remme, J. (2007). Substrate specificity of the pseudouridine synthase RluD in Escherichia coli. *FEBS Journal* 274, 5759-5766.
13. Sumita, M., Desaulniers, J.P., Chang, Y.C., Chui, H.M., Clos, L., 2nd, and Chow, C.S. (2005). Effects of nucleotide substitution and modification on the stability and structure of helix 69 from 28S rRNA. *RNA* 11, 1420-1429.
14. Arnez, J.G., and Steitz, T.A. (1994). Crystal structure of unmodified tRNA(Gln) complexed with glutamyl-tRNA synthetase and ATP suggests a possible role for pseudo-uridines in stabilization of RNA structure. *Biochemistry* 33, 7560-7567.
15. Davis, D.R. (1995). Stabilization of RNA stacking by pseudouridine. *Nucleic acids research* 23, 5020-5026.
16. Newby, M.I., and Greenbaum, N.L. (2001). A conserved pseudouridine modification in eukaryotic U2 snRNA induces a change in branch-site architecture. *RNA (New York, NY)* 7, 833-845.
17. Newby, M.I., and Greenbaum, N.L. (2002). Investigation of Overhauser effects between pseudouridine and water protons in RNA helices. *Proceedings of the National Academy of Sciences of the United States of America* 99, 12697-12702.
18. Spenkuch, F., Motorin, Y., and Helm, M. (2014). Pseudouridine: still mysterious, but never a fake (uridine)! *RNA Biol* 11, 1540-1554.
19. Bykhovskaya, Y., Casas, K., Mengesha, E., Inbal, A., and Fischel-Ghodsian, N. (2004). Missense mutation in pseudouridine synthase 1 (PUS1) causes mitochondrial myopathy and sideroblastic anemia (MLASA). *American journal of human genetics* 74, 1303-1308.
20. Cao, M., Dona, M., Valentino, M.L., Semplicini, C., Maresca, A., Cassina, M., Torracco, A., Galletta, E., Manfioli, V., Soraru, G., et al. (2016). Clinical and molecular study in a long-surviving patient with MLASA syndrome due to novel PUS1 mutations. *Neurogenetics* 17, 65-70.

21. Casas, K.A., and Fischel-Ghodsian, N. (2004). Mitochondrial myopathy and sideroblastic anemia. *Am J Med Genet A* 125A, 201-204.
22. Fernandez-Vizarrá, E., Berardinelli, A., Valente, L., Tiranti, V., and Zeviani, M. (2009). Nonsense mutation in pseudouridylate synthase 1 (PUS1) in two brothers affected by myopathy, lactic acidosis and sideroblastic anaemia (MLASA). *BMJ Case Rep* 2009; 2009, pii: bcr05.2009.1889.
23. Metodiev, M.D., Assouline, Z., Landrieu, P., Chretien, D., Bader-Meunier, B., Guitton, C., Munnich, A., and Rotig, A. (2015). Unusual clinical expression and long survival of a pseudouridylate synthase (PUS1) mutation into adulthood. *Eur J Hum Genet* 23, 880-882.
24. Zeharia, A., Fischel-Ghodsian, N., Casas, K., Bykhocskaya, Y., Tamari, H., Lev, D., Mimouni, M., and Lerman-Sagie, T. (2005). Mitochondrial myopathy, sideroblastic anemia, and lactic acidosis: an autosomal recessive syndrome in Persian Jews caused by a mutation in the PUS1 gene. *Journal of child neurology* 20, 449-452.
25. Shaheen, R., Han, L., Faqeih, E., Ewida, N., Alobeid, E., Phizicky, E.M., and Alkuraya, F.S. (2016). A homozygous truncating mutation in PUS3 expands the role of tRNA modification in normal cognition. *Hum Genet* 135, 707-713.
26. Safra, M., Nir, R., Farouq, D., Vainberg Slutskin, I., and Schwartz, S. (2017). TRUB1 is the predominant pseudouridine synthase acting on mammalian mRNA via a predictable and conserved code. *Genome Res* 27, 393-406.
27. Behm-Ansmant, I., Urban, A., Ma, X., Yu, Y.T., Motorin, Y., and Branlant, C. (2003). The *Saccharomyces cerevisiae* U2 snRNA:pseudouridine-synthase Pus7p is a novel multisite-multisubstrate RNA:Psi-synthase also acting on tRNAs. *RNA* 9, 1371-1382.
28. Guzzi, N., Ciesla, M., Ngoc, P.C.T., Lang, S., Arora, S., Dimitriou, M., Pimkova, K., Sommarin, M.N.E., Munita, R., Lubas, M., et al. (2018). Pseudouridylation of tRNA-Derived Fragments Steers Translational Control in Stem Cells. *Cell* 173,1204-1216.
29. Riazuddin, S., Hussain, M., Razzaq, A., Iqbal, Z., Shahzad, M., Polla, D.L., Song, Y., van Beusekom, E., Khan, A.A., Tomas-Roca, L., et al. (2017). Exome sequencing of Pakistani consanguineous families identifies 30 novel candidate genes for recessive intellectual disability. *Molecular psychiatry* 22, 1604-1614.
30. Abou Jamra, R., Wohlfart, S., Zweier, M., Uebe, S., Priebe, L., Ekici, A., Giesebrecht, S., Abboud, A., Al Khateeb, M.A., Fakher, M., et al. (2011). Homozygosity mapping in 64 Syrian consanguineous families with non-specific intellectual disability reveals 11 novel loci and high heterogeneity. *Eur J Hum Genet* 19, 1161-1166.
31. Seelow, D., Schuelke, M., Hildebrandt, F., and Nurnberg, P. (2009). HomozygosityMapper--an interactive approach to homozygosity mapping. *Nucleic Acids Res* 37, W593-599.
32. Riecken, L.B., Tawamie, H., Dornblut, C., Buchert, R., Ismayel, A., Schulz, A., Schumacher, J., Sticht, H., Pohl, K.J., Cui, Y., et al. (2015). Inhibition of RAS activation due to a homozygous ezrin variant in patients with profound intellectual disability. *Human mutation* 36, 270-278.
33. Motorin, Y., Keith, G., Simon, C., Foiret, D., Simos, G., Hurt, E., and Grosjean, H. (1998). The yeast tRNA:pseudouridine synthase Pus1p displays a multisite substrate specificity. *RNA (New York, NY)* 4, 856-869.
34. Chen, J., and Patton, J.R. (2000). Pseudouridine synthase 3 from mouse modifies the anticodon loop of tRNA. *Biochemistry* 39, 12723-12730.
35. Zhao, X., Li, Z.H., Terns, R.M., Terns, M.P., and Yu, Y.T. (2002). An H/ACA guide RNA directs U2 pseudouridylation at two different sites in the branchpoint recognition region in *Xenopus* oocytes. *RNA* 8, 1515-1525.
36. Hu, Y., Flockhart, I., Vinayagam, A., Bergwitz, C., Berger, B., Perrimon, N., and Mohr, S.E. (2011). An integrative approach to ortholog prediction for disease-focused and other functional studies. *BMC Bioinformatics* 12, 357.
37. Strauss, R., Hanesch, U., Kinkelin, M., Wolf, R., and Heisenberg, M. (1992). No-bridge of *Drosophila melanogaster*: portrait of a structural brain mutant of the central complex. *J Neurogenet* 8, 125-155.
38. Trannoy, S., Chowdhury, B., and Kravitz, E.A. (2015). A New Approach that Eliminates Handling for Studying Aggression and the "Loser" Effect in *Drosophila melanogaster*. *J Vis Exp*, e53395.



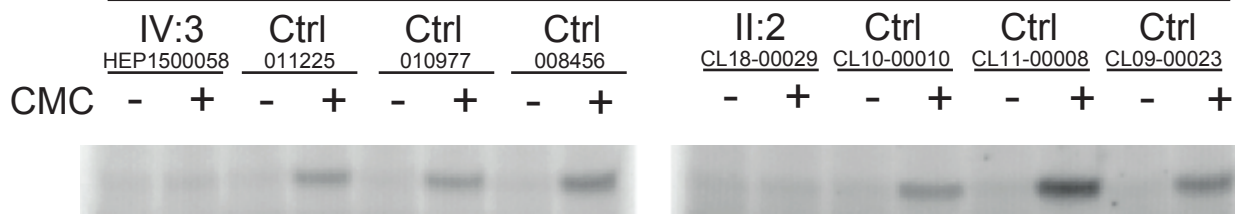
**Table 1.** Overview of clinical data of individuals with a *PUS7* variant. *PUS7* GenBank: NM\_019042.3. CNS=central nervous system; HC=head circumference; MRI=magnetic resonance imaging; ND=not determined; SD are established according to the country of origin. In bold the feature that occur in more than five out of the six affected individuals.

	<b>Family</b>	<b>1 (PKMR215)</b>			<b>2 (MR046)</b>		<b>3 (R14-22173)</b>	<b>Total</b>
	Ethnicity	Pakistani			Syrian		Moroccan	
	mRNA variant	c.89_90del			c.1348C>T		Exon 15 deletion	
	Protein change	p.(Thr30Lysfs*20)			p.(Arg450*)		p.(?)	
	Individual	IV-2	IV-3	IV-4	IV-1	IV-2	II-2	
	Gender	Female	Male	Male	Male	Male	Male	
	Age of last examination	18 yrs	14 yrs	7 yrs	8 yrs	2 yrs	3 yrs 3 mths	
Growth	Birth parameters	Normal	Normal	Normal	'Small' <sup>a</sup>	Normal	Normal	-
	Height (cm)	140 (<-3.9 SD)	137 (<-3.5 SD)	ND	104 (-4.0 SD)	80 (-2.2 SD)	95.5 (-2.2 SD)	<b>5/5</b>
	Weight (kg)	37 (-3.6SD)	29.5 (-3.2 SD)	ND	ND	ND	11.5 (-3.0 SD)	3/3
	HC (cm)	50 (-4.0 SD)	49 (-3.6 SD)	ND	46.5 (-4.5 SD)	46 (-2.5 SD)	46.3 (-2.5 SD)	<b>5/5</b>
Neurological	Intellectual disability (level)	+ (moderate)	+ (moderate)	+ (moderate)	+ (moderate)	+ (moderate)	+	<b>6/6</b>
	Motor delay	-	-	-	+	+	+	3/6
	Speech delay	+	+	+	+	+	+	<b>6/6</b>
	Behavioral problems	Aggressive	Aggressive	Aggressive	Aggressive	ND	Aggressive	<b>5/5</b>
	Seizures	-	-	-	-	-	-	-
Craniofacial	Smooth philtrum	+	+	ND	+	+	+	<b>5/5</b>
	Full lips	+/-	+/-	ND	-	-	+	-
	Everted lower lip	+	+	ND	-	-	+	3/5
	Hypodontia	+	-	ND	-	-	+	2/5
	Conical shaped teeth	-	-	ND	-	-	+	-
CNS	MRI performed	-	-	-	+	-	+	-
	CNS abnormality	ND	ND	ND	Generalized atrophy and enlargement of ventricles	ND	-	1/2
	Other	-	-	-	Hepatomegaly	-	-	-

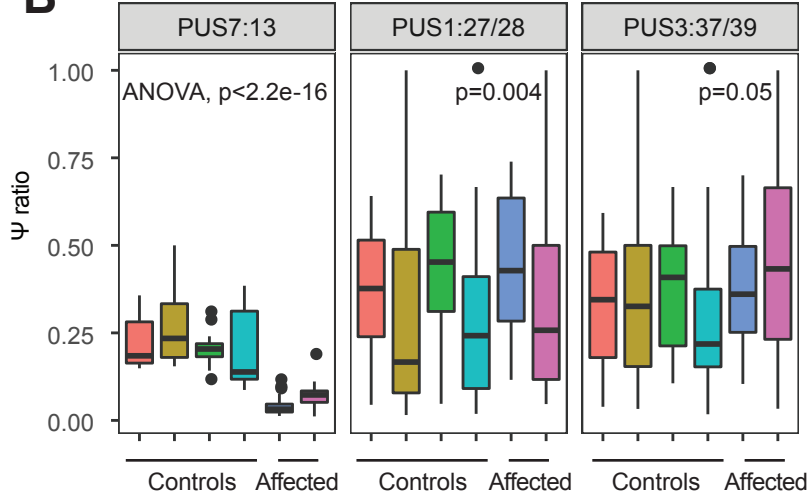
<sup>a</sup> As reported by the parents

cyto-tRNA-Glu

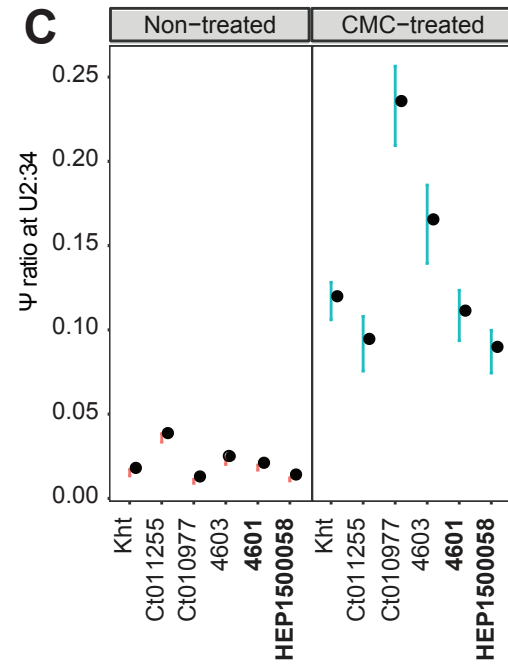
**A**



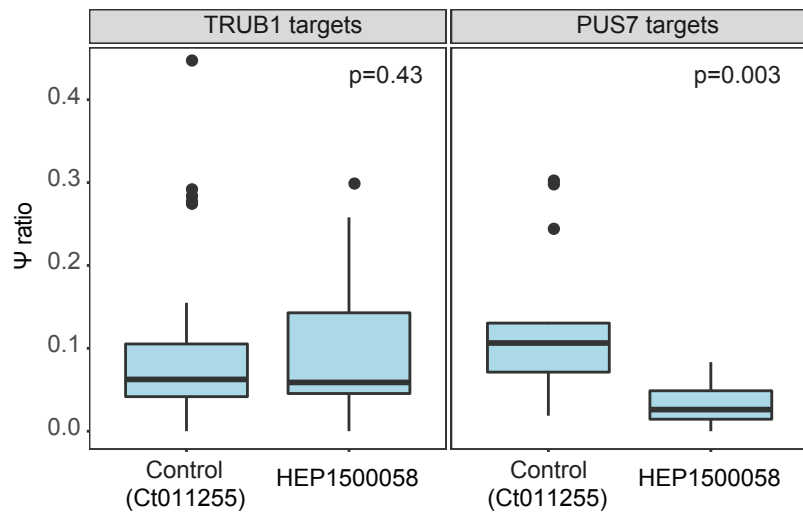
**B**



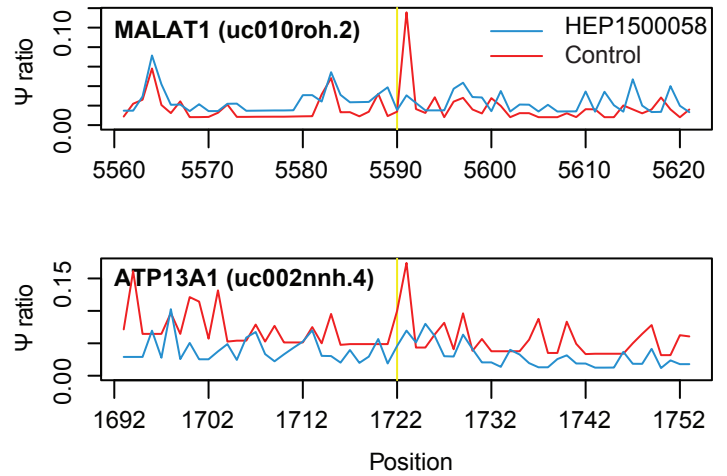
**C**

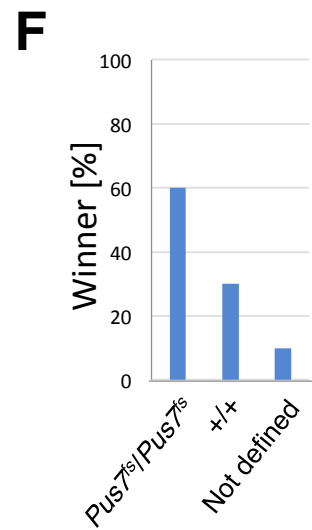
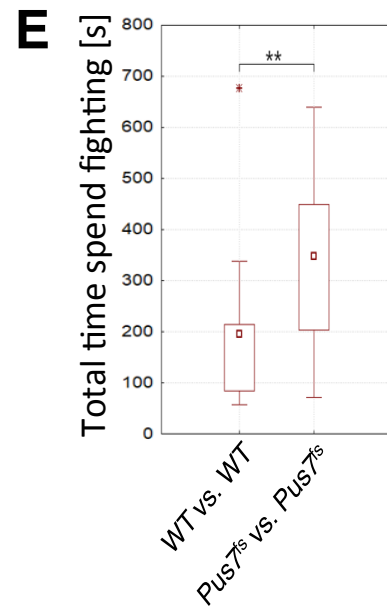
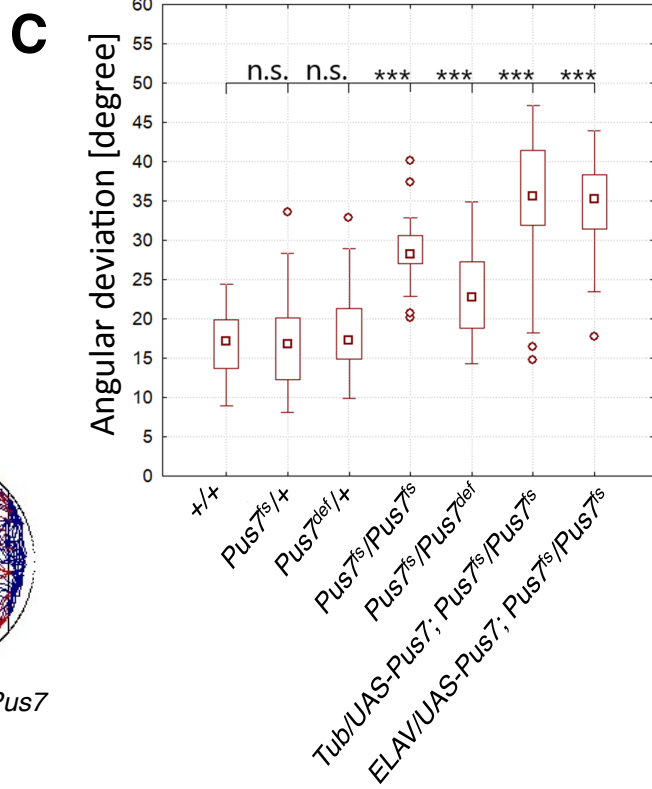
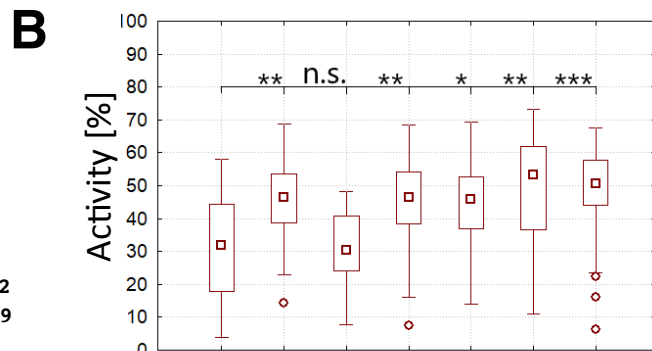
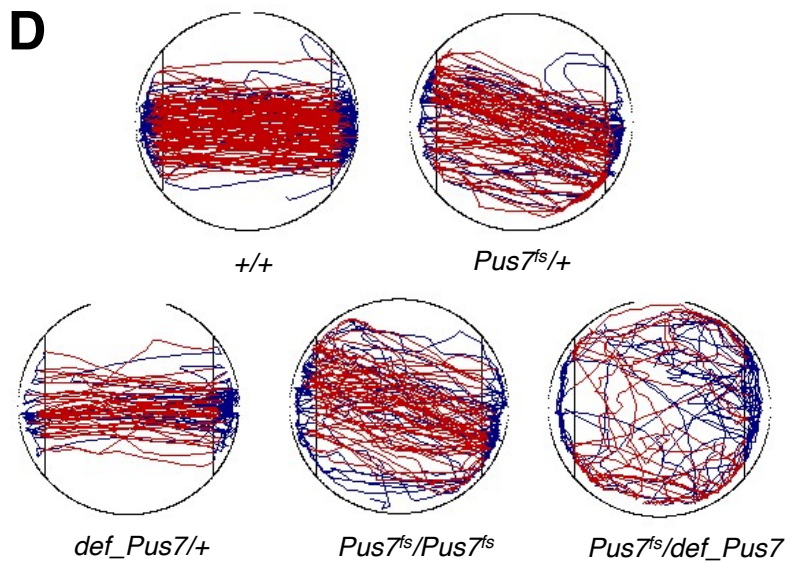
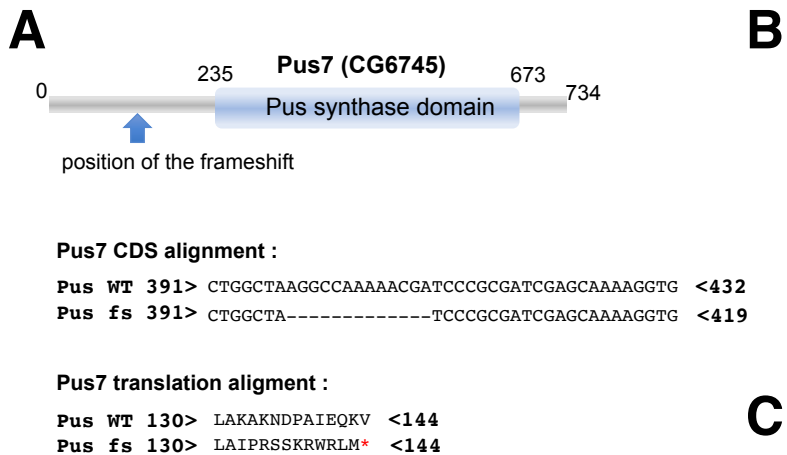


**D**



**E**





## Supplemental Note: Case Reports

### *Family 1 (PKMR215)*

Family 1 (PKMR215; **Fig. 1A; Table 1**) originates from Pakistan and has been described briefly before by Riazuddin *et al.* (2016)<sup>4</sup> as a family with moderate ID, speech delay and aggressive behavior. The parents of the four affected siblings are first cousins. Pregnancy and delivery were uneventful and birth parameters within normal range. At the time of investigation, the oldest affected daughter was 18 years-old. Her body weight was 37 kg (-3.6 SD), her length 140 cm (-3.9 SD), and head circumference 50 cm (-4.0 SD). Her younger brother weighed 29.5 kg (-3.2 SD), measured 137 cm (-3.5 SD), and had a head circumference of 49 cm (-3.6 SD) at the age of 14 years. This indicates that both siblings have microcephaly and short stature. Both affected siblings have abnormal dentition. Family member IV:2 has hypodontia and misaligned teeth while IV:3 has only misaligned teeth. In addition, both siblings have a smooth philtrum and an everted lower lip (**Fig. 1A**). There were two other affected children in this family. A 10 year old affected male child, IV:4, of this family was adopted by their relatives and is not living with them anymore. The affected daughter IV:5 died at the age of five years of uncertain causes.

### *Family 2 (MR046)*

Family 2 (MR046; **Fig. 1B; Table 1**) is from the Southern part of Syria. The parents are first degree cousins. They have two sons with a moderate intellectual disability. Pregnancies of both children were uneventful. The parents reported that at birth the elder boy (IV-1) had a small head, and that he seemed to be lifeless for the first 30 minutes after birth. He crawled at the age of 3-4 years and walked at the age of 5 years. At the time of examination, he was 8 years old, was 104 cm tall (-4.0 SD), and had a head circumference of 46.5 cm (-4.5 SD). He did not talk, and he showed aggressive (beats other children) and destructive behavior (destroying furniture of examination room). He permanently tried to provoke his parents and grandfather. Abdomen ultrasound showed that liver was mildly enlarged. Liver biopsy, bone age measurement and eye examination were unremarkable. Brain MRI revealed mild atrophy and enlargement of ventricles.

The pregnancy, birth and neonatal phase of the younger affected child (IV-2) was unremarkable. At the time of examination, he was two years old, was 80 cm tall (-2.2 SD), and had a head circumference of 46 cm (-2.5 SD). He could not walk, but he was sliding forward on his bum. He also did not talk. He had anemia and ferritin levels were decreased. Both boys have some remarkable facial characteristics of long and smooth philtrum, thin lips with down-slanting palpebral fissures, and arched eyebrows (**Fig. 1B**). None of the boys had epilepsy. Sleeping pattern, hearing and vision of both seemed to be unremarkable.



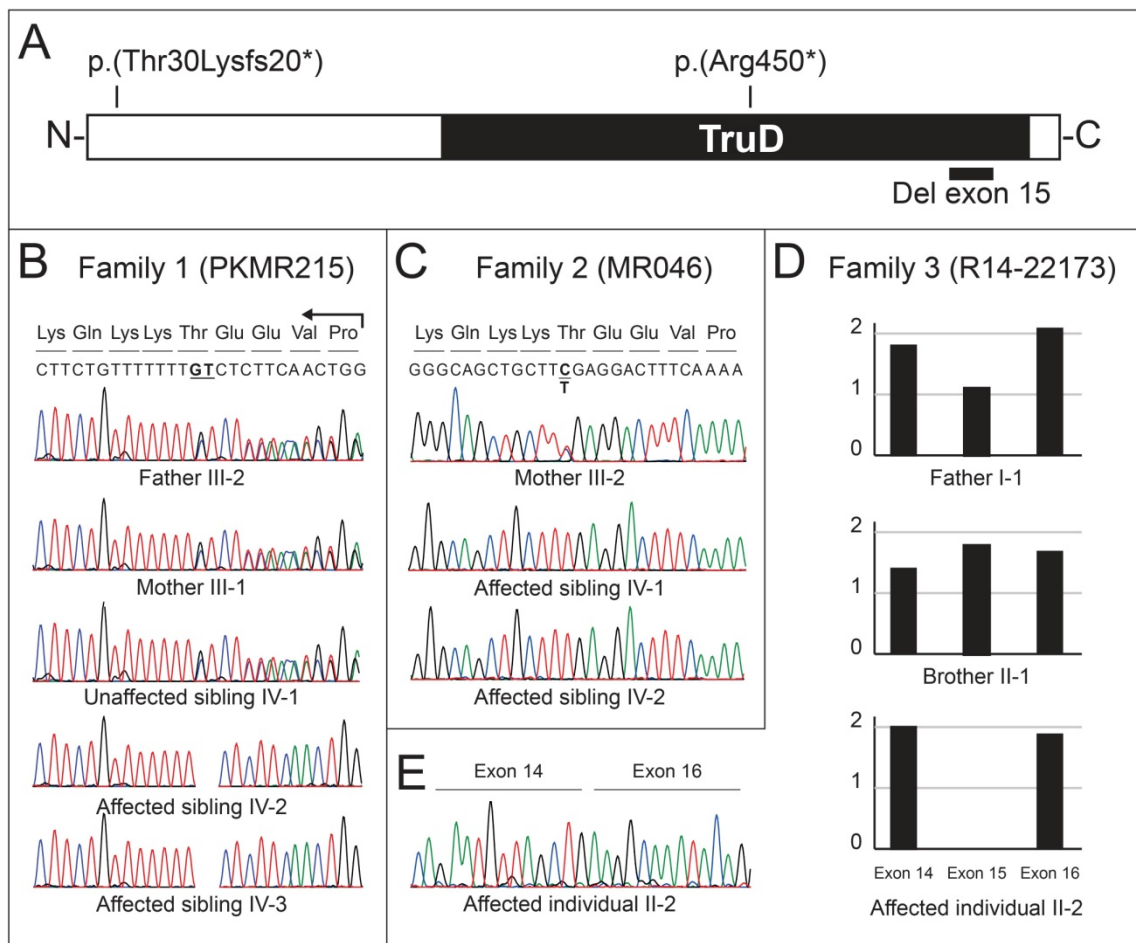
### *Family 3 (R14-22173)*

Family 3 (R14-22173) is a consanguineous Dutch family of Moroccan descent in which one boy has intellectual disability (**Fig. 1C; Table 1**). He has an older brother with speech delay only. The affected individual was born at 40+1 weeks of gestation to healthy consanguineous parents who were first cousins. Pregnancy was uneventful. The birth weight was 3440 grams and the APGAR score was 7 and 9 at 1 and 5 minutes after birth. The neonatal period was complicated by feeding difficulties and hypopnea, requiring tube feeding and respiratory support for three weeks. At 4 months of age plagiocephaly and axial hypotonia was noticed with head lag and slipping through. His height was 62 cm (-0.4 SD), weight 6.2 kg (-0.22 SD), and head circumference 40.2 cm (-1.3 SD). Serum analysis revealed elevated levels of lactate, alanine and transaminases, so a mitochondrial disorder was suspected. Echography of the heart and liver were normal and also a MRI of the brain did not reveal any abnormalities. The muscle biopsy at age 7 months showed no significant pathologic changes, except for the mild reduction in skeletal muscle oxidative ATP + CrP production from pyruvate (13.8 nmol/h.mUCS; reference 15.4-30.2 nmol/h.mUCS). He underwent bilateral orchiopexy for cryptorchidism and an adenotomy.

Global developmental delay was evident from birth. At one year and five months he could pull to stand, cruise along furniture, and sit with support for five minutes. His head balance, however, was still unstable. He could walk independently from age 21 months although unstably and he fell frequently. At the age of three years and three months, he could speak only a few words. He is active, short-tempered, and displays aggressive rebellious behavior with screaming, hitting the wall with his head, and deliberately hitting himself and others.

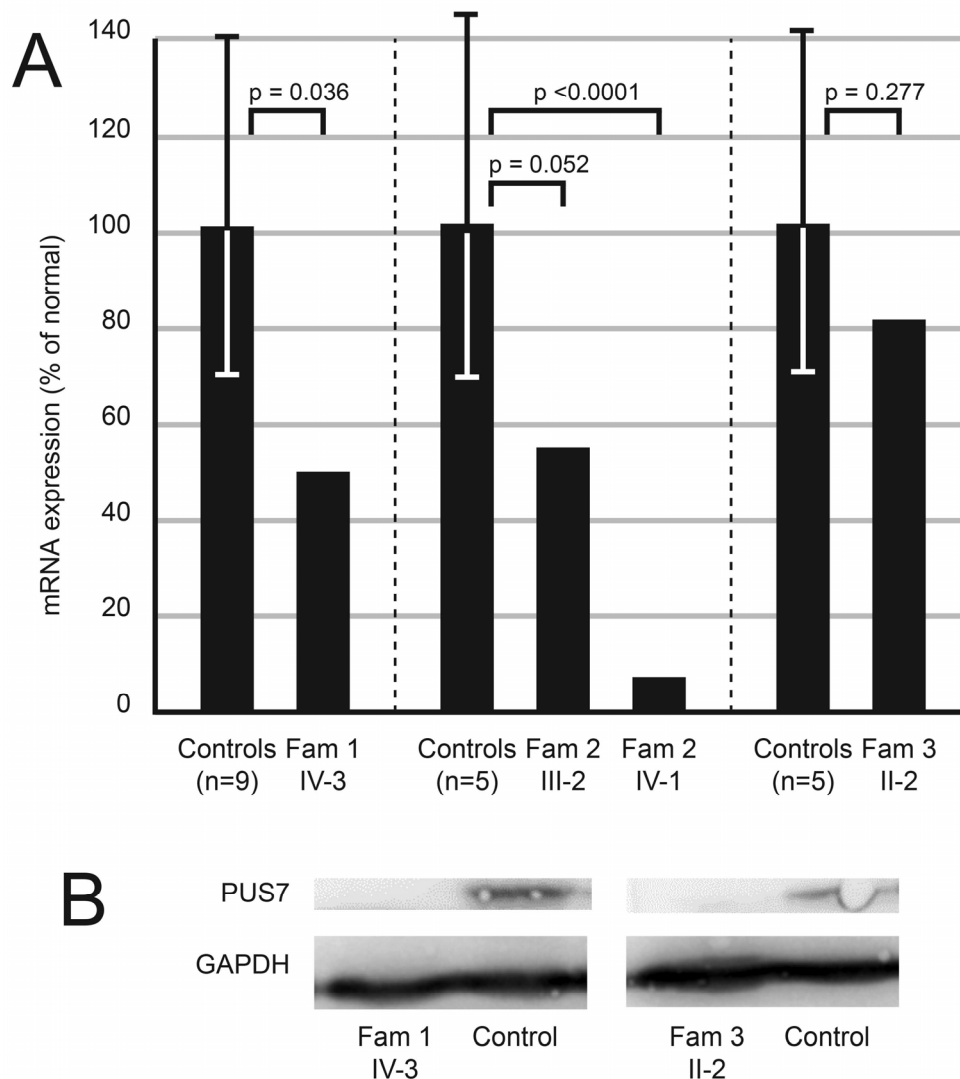
At three years and three months his height is 95.5 cm (-2.2 SD), weight 11.5 kg (-3.0 SD corrected for height), and head circumference 46.3 cm (-2.5 SD). There are no gross facial dysmorphisms, except for bilateral epicanthal folds, broad nasal root, full lips and eversion of lower lip and wide spaced conical shaped teeth (**Fig. 1C**). He has clinodactyly digiti V of the hands and hyperlaxity in the thumbs. Feeding remains problematic. It is difficult to get him to eat. He refuses food and everything has to be mashed.

**Figure S1.** Schematic representation of PUS7 and molecular genetic analysis confirming the *PUS7* variants.



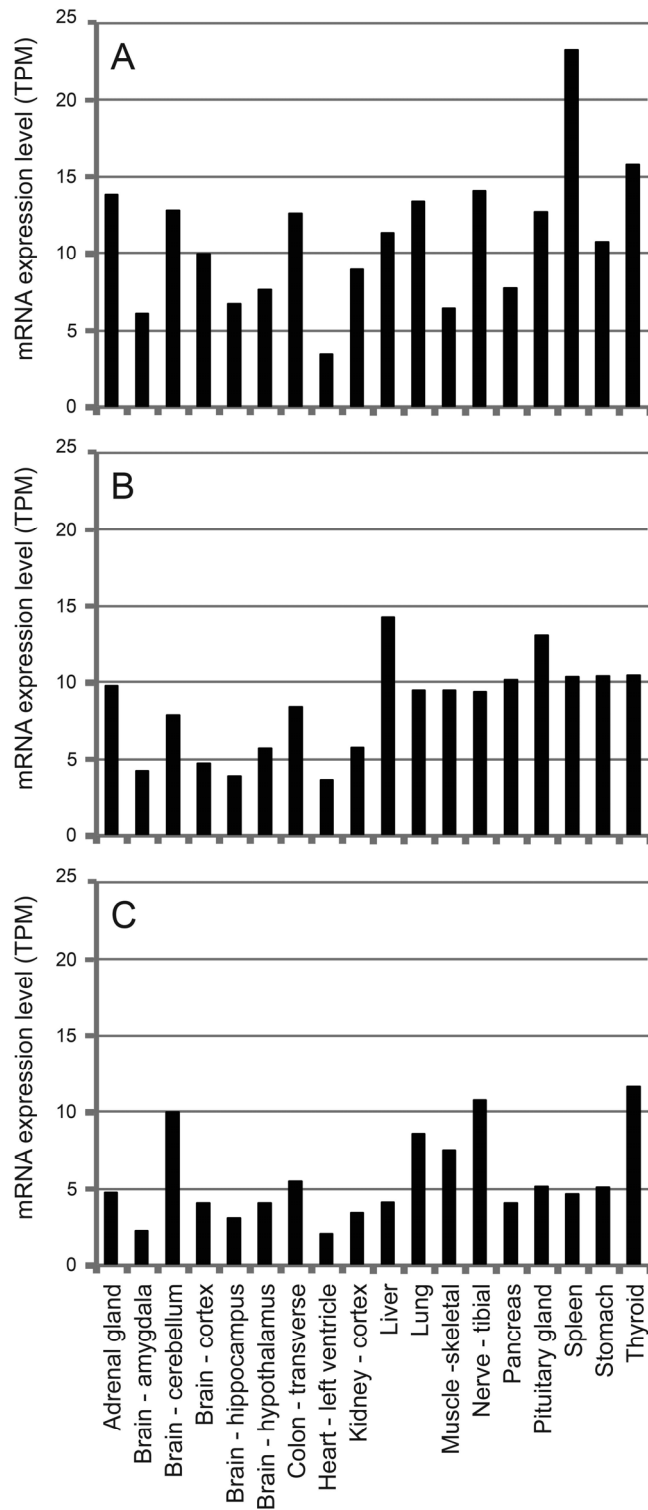
**A)** The upper panel shows a schematic representation of human PUS7 with the positions of three mutations identified. The black box represents the TruD domain, the catalytic domain involved in pseudouridylation. **B)** Electropherograms of *PUS7* in family 1 showing the presence of the c.89\_90del frameshift variant in the father, mother, and the two affected siblings. The arrow indicates the direction in which the protein is translated. **C)** Electropherograms of *PUS7* in family 2 showing the presence of the c.1348C>T nonsense variant in the father, mother, and the two affected brothers. **D)** MAQ analysis of exon 14-16 of *PUS7* in family 3 indicating a homozygous deletion of exon 15 in the affected male individual. Mutated nucleotides are printed in bold and underlined. **E)** RT-PCR analysis of the *PUS7* mRNA transcript of individual II-2 from family 3. The electropherogram shows that exon 15 is not present anymore.

**Figure S2.** Effect of human *PUS7* variants on mRNA and protein levels.



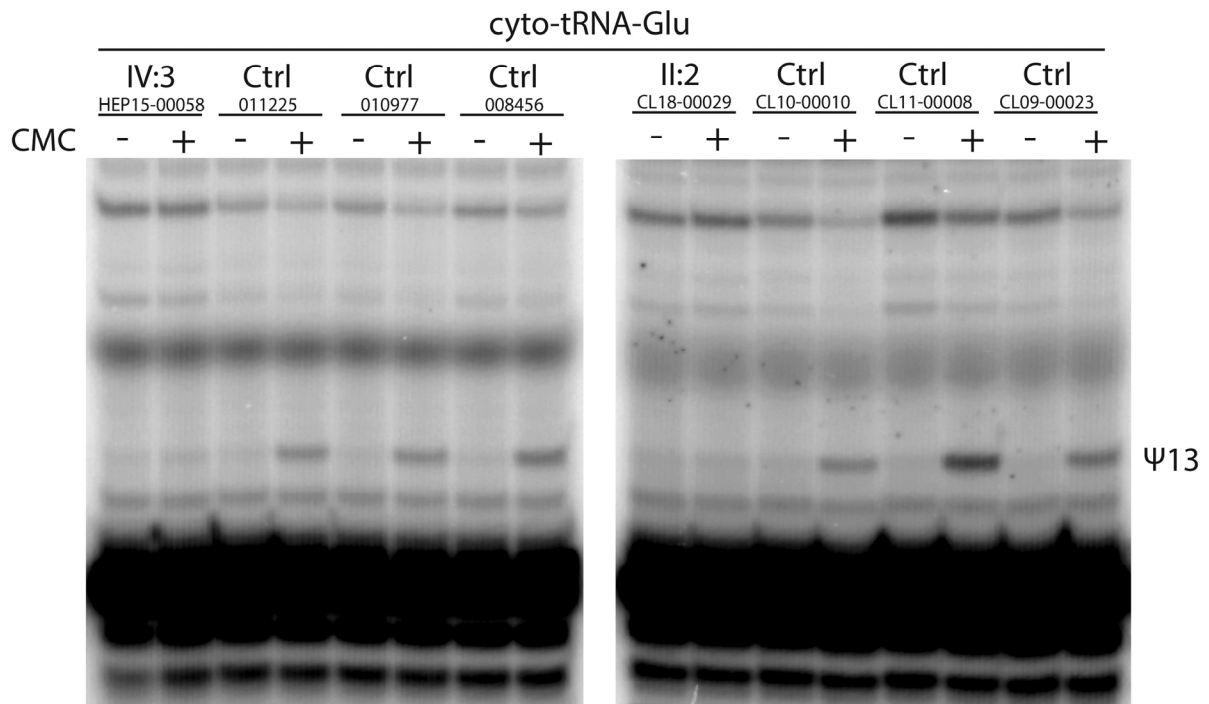
**A)** Effect of the c.89\_90del frameshift (p.(Thr30Lysfs\*20); family 1), c.1348C>T (p.(Arg450\*); family 2), and the deletion of exon 15 (family 3) on *PUS7* expression. Shown are the *PUS7* mRNA expression level in EBV-LCLs of affected family member IV-3 of family 1, affected family member IV-1 of family 2, and his mother III-2, as compared to the mean expression level of *PUS7* in nine or five controls respectively. For family 3, *PUS7* mRNA expression levels in fibroblasts from affected family member II-2 were compared to the mean expression level of fibroblasts from five healthy individuals. **B)** Corresponding Western blot analyses for affected family member IV-3 from family 1 and II-2 from family 3.

**Figure S3.** Expression of *PUS1*, *PUS3*, and *PUS7* in selected human tissues.



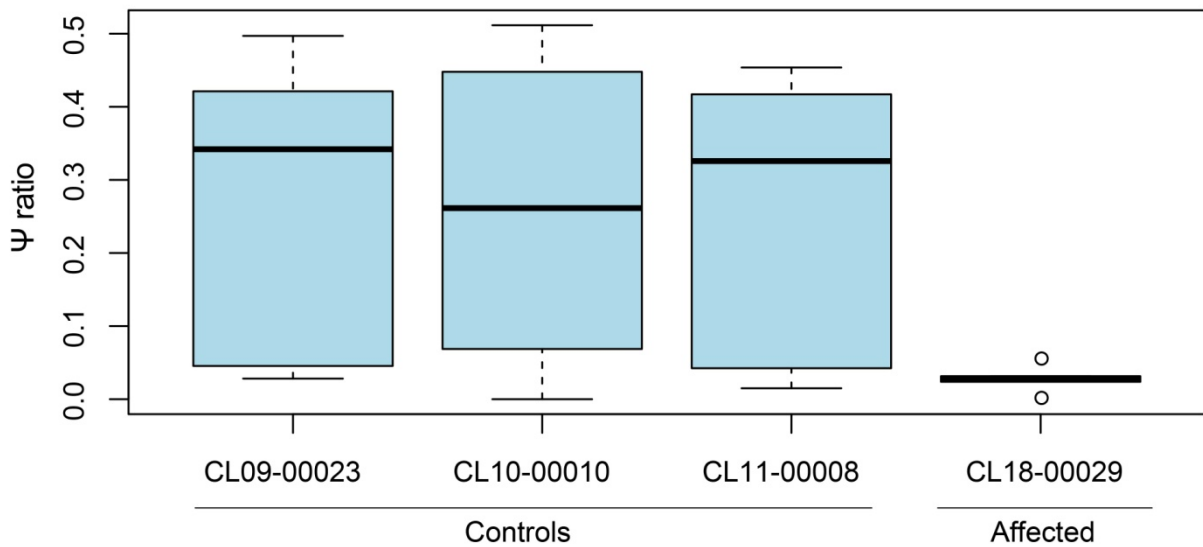
**A) *PUS1*, B) *PUS3*, and C) *PUS7*** expression levels as determined by RNA sequencing. Transcriptome data was retrieved from the Genotype-Tissue Expression (GTEx) project.<sup>21</sup> Levels are given in transcripts per million (TPM).

**Figure S4.** Full gels forming the basis for Figure 2A.



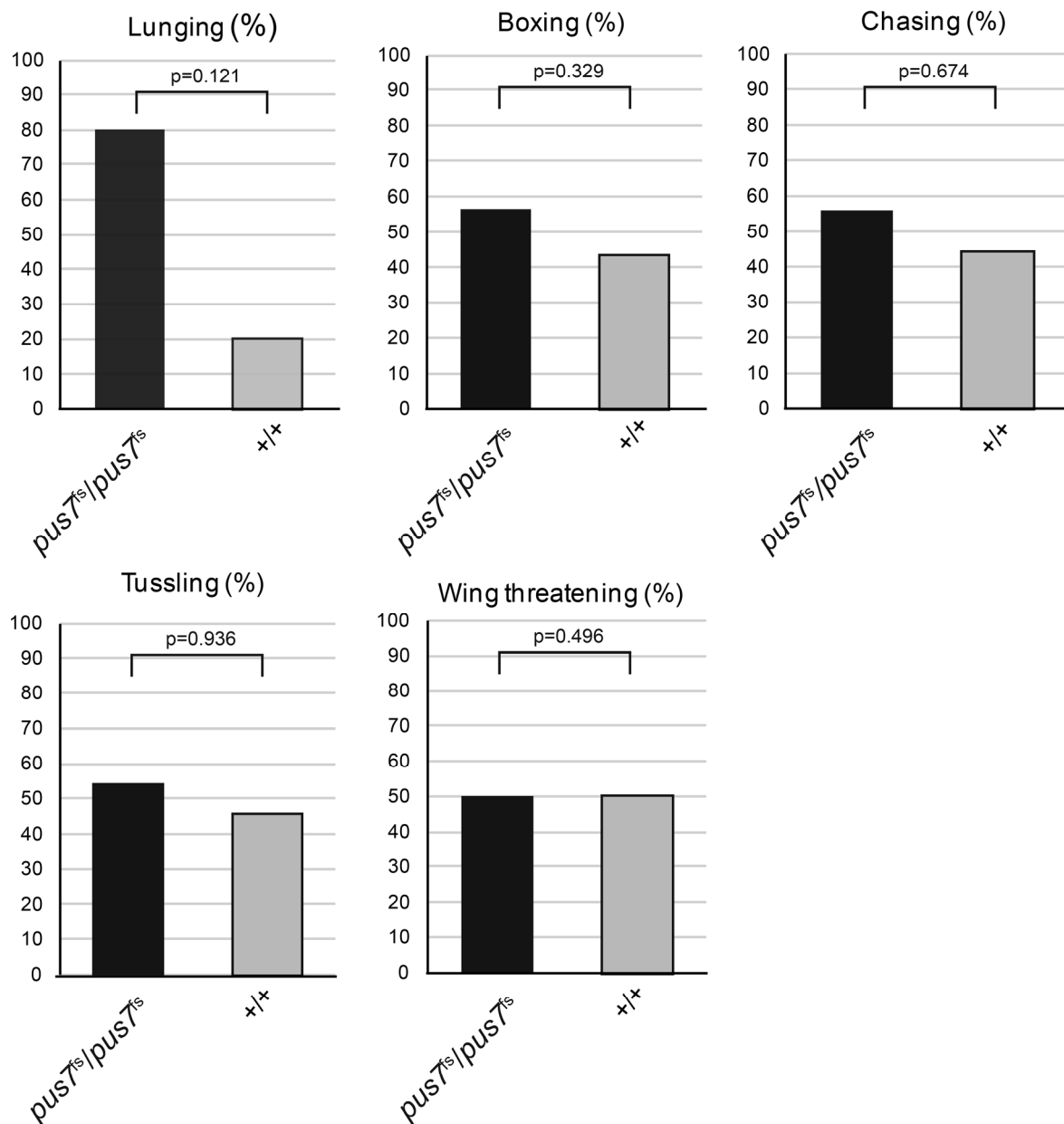
Primer extension analysis against human cytoplasmic tRNA-Glu applied to total RNA extracted from lymphoblasts (IV:3 and corresponding controls) and fibroblasts (II:2 and corresponding controls),

**Figure S5.** Distribution of  $\Psi$ -ratios at position 13 of tRNAs.



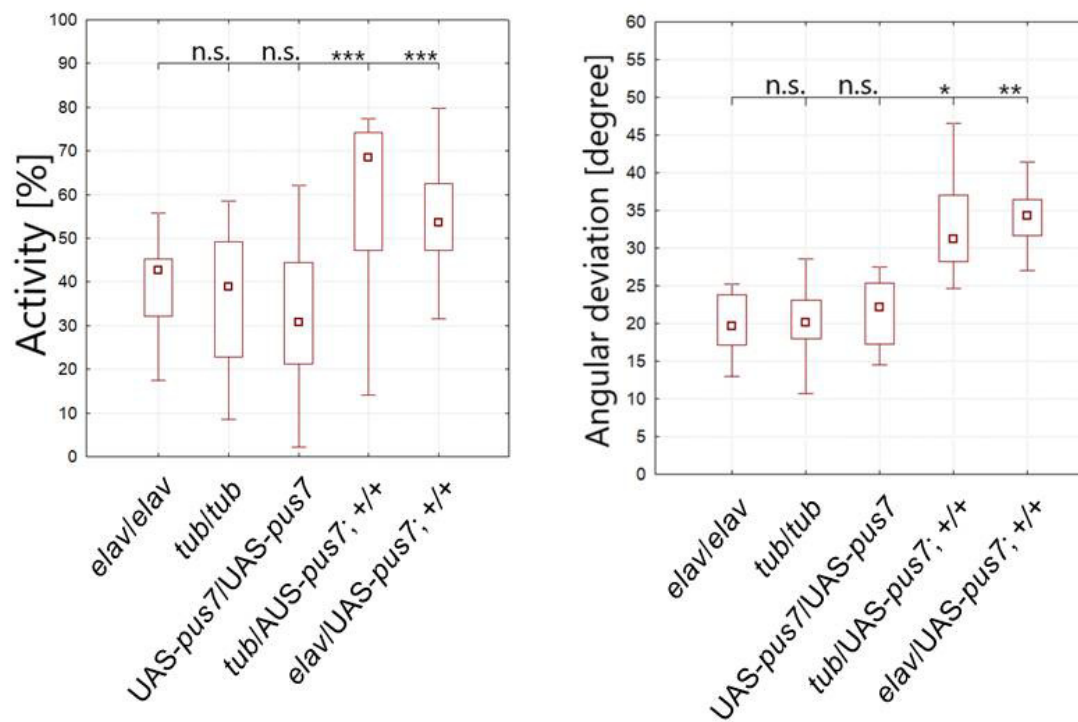
Distribution of  $\Psi$ -ratios at position 13 of tRNAs, measured in primary fibroblasts of affected individual II-2 from family 3. The positions for which values are shown are the ones indicated in **Table S1**, which were identified based on unbiased analysis of affected individuals and controls from family 1. The distributions of the values in the sample of individual II-2 (CL18-00029) from family 3 are significantly different from all three controls (paired t-test,  $p$ -value $<0.05$  for all three pairwise comparisons).

**Figure S6.** Effect of *pus7* knockout on aggressive behavior in *Drosophila melanogaster*.



Interactions specific for aggressive fly behavior evaluated for fights between wild-type Canton-S and homozygous *pus7<sup>fs</sup>* flies. Shown are the number of interactions per 20 min in % for lunging, boxing, chasing, tussling and wing threatening. Shapiro Wilk test was used to test for normal distribution in each group. The not normal distributed groups were tested by Mann Whitney U test. A lunge is defined as a fly rearing up on its hind legs and snapping down on the opponent.<sup>22; 23</sup> Tussling is defined as two flies wrestle with each other with their front legs. Boxing interactions are characterized as striking the opponent with front legs.<sup>24; 25</sup> Wing threatening is defined as raising both wing by a 45° angle. Chasing is characterized by a fly running after its opponent.

**Figure S7.** Pus7 overexpression alters fly activity and orientation.



Walking behavior of *pus7* mutant flies in Buridan's paradigm. Activity (left) and Median angular displacements from the direct approach to one of the stripes (right) were monitored. Thirty flies (15 males and 15 females) were tested per genotype. Three control conditions were used (*elav/elav*, *tub/tub* and *UAS-pus7/UAS-pus7*). Behavior of flies overexpressing *pus7* ubiquitously (*tub/UAS-pus7; +/+*) or only in neurons (*elav/UAS-pus7; +/+*) are shown. NS, not significant; \*  $p < 0.05$ , \*\*  $p < 0.01$ , \*\*\*  $p < 0.001$  (t-test analysis of variance with Bonferroni correction).



**Table S1.** Differentially pseudouridylated sites between affected individuals and controls.

UCSC id	geneSymbol	Pos	seq	Kht	Ct011255	4603	Ct010977	4601	HEP1500058
uc021roj.1	TRNA_Pro	13	TCTAG	0.16	0.17	0.18	0.12	0.02	0.03
uc021ouu.1	TRNA_His	13	TATAG	0.18	0.17	0.17	0.12	0.04	0.07
uc021zep.1	TRNA_Glu	13	TCTAG	0.32	0.43	0.21	0.31	0.04	0.05
uc021unh.1	TRNA_Gly	13	TATAG	0.16	0.15	0.18	0.10	0.03	0.01
uc021ouv.1	TRNA_Gly	13	TATAG	0.25	0.40	0.28	0.31	0.03	0.08
uc021ymf.1	TRNA	13	TGTAA	0.29	0.22	0.30	0.35	0.03	0.03
uc021tpz.1	TRNA_Gly	13	TATAG	0.16	0.18	0.20	0.13	0.02	0.02
uc021rbz.1	TRNA_Asp	13	TATAG	0.26	0.22	0.22	0.38	0.11	0.08
uc021rjd.1	TRNA	13	TCTAG	0.18	0.26	0.21	0.09	0.02	0.07
uc021rcj.1	TRNA_Asp	13	TATAG	0.18	0.22	0.24	0.14	0.05	0.06

$\Psi$ -ratios across all six monitored samples across all sites that were detected as significantly different (both t-test p-value <0.05 and chi-squared p-value <0.05) in the two affected individuals, compared to the four controls. For each site we provide its UCSC ID and corresponding genesymbol, the putative pseudouridine site, the sequence in a window of 5 bp surrounding the modified site, and the  $\Psi$ -ratios across the different samples.

**Table S2.** Putative Pus7 substrates within human mRNAs.

<b>Genomic coordinates</b>	<b>Transcriptomic coordinates</b>	<b>geneSymbol</b>	<b>strand</b>	<b>seq</b>
chr11:65270823	uc010roh.2:5591	<i>MALAT1</i>	+	TGTAG
chr19:572612	uc002loz.3:76	<i>BSG</i>	+	TGTAG
chr19:19765470	uc002nnh.4:1723	<i>ATP13A1</i>	-	TGTAG
chr1:16861832	uc021ogr.1:313	<i>BC036435</i>	-	TCTAG
chr15:41059798	uc001zmr.1:600	<i>GCHFR</i>	+	TGTAG
chrX:48681764	uc004dks.1:3048	<i>HDAC6</i>	+	TGTAG
chr11:60690725	uc001nqg.3:2198	<i>TMEM109</i>	+	TCTAG
chr12:7053219	uc001qrw.1:6086	<i>ATN1</i>	+	TGTAG
chr1:173837116	uc001gjk.3:10	<i>GAS5</i>	-	GGTAG

For each substrate we list its genomic and transcriptomic coordinates, its gene symbol and strand, and a sequence of five bases centered around the putative pseudouridylation site.

**Table S3.** Putative Pus7 substrates in *Drosophila*.

Coordinates	del	WT	del	WT	Chi-squ.	t-test	5-bp	21 bp
chr3L.trna31-ProCGG:13	0.03	0.01	0.03	0.34	5.5E-60	4.7E-07	TCTAG	CTCGTTGGTCTAGAGGTATGA
chr2R.trna25-GluCTC:13	0.00	0.00	0.01	0.11	4.9E-199	5.8E-04	TCTAG	CCATATTGTCTAGTGGTTAGG
chr2L.trna18-ProAGG:13	0.01	0.01	0.02	0.29	6.5E-24	1.6E-04	TCTAG	CTCGTTGGTCTAGGGGTATGA
chr3R.trna24-GlyTCC:13	0.00	0.00	0.02	0.26	4.6E-61	3.3E-03	TGTAA	GTCGGTGGTGTAAATGGTTAGC
chr2R.trna26-GluTTC:13	0.01	0.00	0.01	0.25	6.7E-59	4.1E-03	TCTAG	CCATATGGTCTAGTGGCTAGG
chr2L.trna12-AspGTC:13	0.00	0.00	0.01	0.04	2.9E-86	5.9E-06	TATAG	CTCGATAGTATAGTGGTTAGT
chr2L.trna2-GlnCTG:13	0.01	0.00	0.01	0.30	8.5E-17	3.1E-03	TGTAA	TTCCATGGTGTAAATGGTTAGC
chr3R.trna17-ProTGG:13	0.01	0.01	0.03	0.27	9.0E-19	5.8E-03	TCTAG	CTCAATGGTCTAGGGGTATGA
chr2L.trna8-AspGTC:20	0.02	0.02	0.04	0.12	1.0E-06	6.7E-03	GTTAG	GTATAGTGGTTAGTATCCCCG
chr3R.trna24-GlyTCC:11	0.02	0.03	0.04	0.08	1.3E-03	4.3E-02	GGTGT	GCGTCGGTGGTGTAAATGGTTA
chr2L.trna38-GlnCTG:13	0.02	0.00	0.00	0.18	9.5E-05	9.0E-02	TGTAA	TTCTATGGTGTAAATGGTTAGC

For each substrate, we list its coordinate, the aggregate stop ratio achieved across four wild-type (WT) and four *pus7* deletion (del) replicates in either CMC-treated samples or Input (non-treated samples), and t-test and chi-squared (Chi-squ.) derived p-values comparing assessing the significance of the comparison between wild-type and deletion samples. We further provide the sequence surrounding the identified site.

## Supplemental Methods

### *Exome sequencing & CNV analysis*

Genomic DNA was isolated from peripheral blood samples following standard procedures.<sup>3</sup> Exome enrichment and high-throughput sequencing were performed at the Radboudumc (Nijmegen, the Netherlands), The Wellcome Trust Sanger Institute (Hinxton, UK; as part of the UK10K study), and the Institute of Human Genetics (Erlangen, Germany) as previously described.<sup>2; 4</sup> Copy number variant analysis was either performed on exome data by using CoNVex<sup>5</sup> (Family 1; Wellcome Trust Sanger Institute, Hinxton), on Illumina SNP chip data by standard Illumina software (Family 2; Institute of Human Genetics, Erlangen), or by chromosome microarray analysis using the Affymetrix CytoScan HD array platform and on exome data by using CoNIFER<sup>6</sup> as described before<sup>7</sup> (Family 3; Radboudumc, Nijmegen). Selection of biallelic potentially pathogenic variants was performed using seven major filtration steps as previously described.<sup>4; 8</sup> In case of family 3, a *de novo* analysis was performed as well by established procedures.<sup>9</sup>

### *Sanger sequencing*

Validation of variants and sequencing of the coding exons of *PUS7* (GenBank: NM\_019042.3) was performed using Sanger sequencing. Primer sequences and conditions for PCR are available upon request. PCR products were sequenced using the ABI PRISM BigDye Terminator Cycle Sequencing V2.0 Ready Reaction Kit and analysed with the ABI PRISM 3730 DNA analyzer (Applied Biosystems, Foster City, USA). DNA of all available family members was analyzed for the variant found in the proband to confirm the segregation of the variant with the disease. Nucleotide numbering uses +1 as the A of the ATG translation initiation codon in the reference sequence, with the initiation codon as codon 1.

### *Multiplex amplification quantification*

Multiplex amplification quantification (MAQ) was essentially performed as described by Kumps *et al.*<sup>10</sup> Custom-made probes were designed for exons 14, 15, and 16. Their signal was compared to the average signal of six control probes located elsewhere in the genome of three healthy control individuals consisting of two women and one man. All probe sequences are available on request.

### *Quantitative and reverse transcriptase PCR analysis*

Quantitative PCR (QPCR) analysis to assess nonsense-mediated mRNA decay of mutated *PUS7* in human Epstein Barr-Virus-transformed lymphoblastoid cell lines (EBV-LCLs) and fibroblasts was performed as described before.<sup>11</sup> Reverse transcriptase PCR (RT-PCR) analysis was executed as described by Vulto-van Silfhout et al. (2015).<sup>12</sup>

### *Western blot*

A similar number of cells from different affected individuals were lysed using standard lysis buffer with protease inhibitor cocktail (Calbiochem, Merck KGaA, Darmstadt, Germany). Proteins were separated using standard PAGE separation, transferred to a nitrocellulose membrane and detected by western blotting as described previously.<sup>13</sup> The following antibodies were used: anti-GAPDH (dilution 1:2000; Sigma-Aldrich, Merck KGaA, Darmstadt, Germany), anti-PUS7 (dilution 1:500; Sigma-Aldrich) and secondary HRP anti-rabbit/mouse from Jackson (dilution 1:10,000; ImmunoResearch, West Grove, PA, USA).

### *Transcriptome-wide pseudouridylation analysis*

Total RNA was isolated from EBV-LCLs or from fibroblasts by using QIAzol according to the supplier's instructions (QIAGEN, Hilden, Germany).  $\Psi$ -seq was performed essentially as described previously.<sup>14</sup> Poly(A) enrichment was performed using Oligo(dT) dynabeads (Invitrogen) according to the manufacturer's protocol. Reads were mapped to the human genome using STAR aligner.<sup>15</sup> Putative  $\Psi$  sites in the first set of libraries used to quantify pseudouridine on tRNAs were identified as described in Schwartz *et al.*<sup>14</sup> Firstly, (1) for each treated or non-treated sample, a  $\Psi$ -ratio was calculated, corresponding to the number of reads beginning at the position divided by the overall number of reads covering it. A pseudocount of 1 was added to both the numerator and denominator to stabilize the ratio and avoid division by 0. (2) The  $\Psi$ -fold change was calculated as  $\log_2$  fold changes of  $\Psi$  ratios in the treated versus non-treated samples. All positions with a  $\Psi$ -ratio  $>0.1$ , a  $\Psi$ -fc  $>3$  (8-fold enrichment) and with  $>5$  reads beginning at the position were considered putative  $\Psi$  sites. (3) To compare across conditions, we first merged the positions of all windows passing step (2) from all samples, to define a set of all unique sites passing the filters in at least one condition. For each such site, we then calculated a  $\Psi$ -ratio and  $\Psi$ -fc in each sample. (4) We then performed two statistical tests to assess the difference in pseudouridylation signal between affected individuals and controls. First, we aggregated the number of reads stopping or overlapping but not stopping at each putative position in affected individuals versus controls, and used this as a basis for a chi-squared test. Second, we performed a t-test, comparing the distribution of  $\Psi$ -ratio in affected individuals versus controls. Sites were considered significant if they matched all of the following criteria: (i) chi-squared and t-test p-values  $<$

0.05, (ii) mean  $\Psi$ -ratio in the control >5%, and (iii) Mean  $\Psi$ -fc in the control exceeding 2.5. (5) From the final set of sites we excluded sites not harboring a 'T' at the identified position and eliminated redundant sequences, sharing a 21-bp sequence surrounding the putative target site, in order to retain only a single copy of redundant sequences such as identical tRNA copies. The sites passing these thresholds were also used to visualize  $\Psi$ -ratios across the four fibroblast-derived samples from one affected individual and three controls (**Suppl. Fig. 4**).

For the second set of libraries aiming to quantify pseudouridine on mRNA, an initial catalog of putative high-confidence pseudouridylation sites was obtained from Safra et al.<sup>16</sup> Specifically, we first identified all high confidence sites that were ranked in the two highest classes (classes 5 and 6),<sup>16</sup> based on which we assembled a set of 94 sites harboring a loosely defined TRUB1 motif (GUUC, bold U is the pseudouridylated motif) and 53 sites harboring a Pus7 motif (defined as U[G/A/C]UAG). We then quantified the  $\Psi$ -ratios at each of these sites across the two poly(A) libraries. To ensure adequate quantification and minimal evidence for pseudouridylation in our samples, we only retained sites covered by >15 reads across both samples, and harboring  $\Psi$ -ratios of >3% in at least one of the two samples. This resulted in nine and 25 sites, harboring PUS7 and TRUB1 consensus motifs, respectively. We refer to all relative positions in tRNA based on the standard tRNA nomenclature so that the anticodon nucleotides are always numbered 34–36, and the T loop between positions 54 and 60.

#### *Pseudouridylation analysis in Drosophila*

To confirm that the targets of Pus7 pseudouridylation are conserved in *Drosophila*, we performed  $\Psi$ -seq on total RNA obtained from fly heads, with four replicates per wild-type and *pus7* knockout samples. Two hundred ng of total RNA was used per condition. Reads were aligned against a database comprising a single copy of the *drosophila* rRNA, snRNA and tRNA sequences obtained from FlyBase. Unbiased pseudouridylation analyses were performed as above, with  $\Psi$ -ratio and  $\Psi$ -fc calculated for each position across each of the samples. t-test-based and chi-squared p-values were calculated for each site, comparing the four wild-type samples to *pus7* knockout. Sites were considered as differentially pseudouridylated, if they met the following criteria: (1) Chi-squared p-value <0.05, (2) t-test p-value <0.1, (3)  $\Psi$ -ratio in deletion samples <4%, and (4) difference between aggregated  $\Psi$ -ratio in wild-type versus knock-out >3%. *Drosophila* pseudouridylation sequencing data was deposited in Gene Expression Omnibus (GEO), accession GSE121177.

### *Primer extension analysis*

Total RNA extracted from lymphoblasts and fibroblasts was subjected to CMC/alkaline treatment followed by reverse transcription primer extension, as described previously.<sup>17</sup> The extended primer, 5'-GTGAGAGCGCCGAATCCTAACC-3', targets human cytoplasmic tRNA-Glu.

### *Buridan's behavioral paradigm analysis in Drosophila*

*Drosophila melanogaster Canton-S* with a mutant allele for *pus7* was generated using the CRISPR-Cas9 system, as described previously.<sup>18</sup> Guide RNAs sequences used were GTTTTTGGCCTTAGCCAGAT and GGAGTCGATTTTCAAGCGAA. A deletion of 13bp was produced from basepair 600 to 612 in the genome region chr3L:8,510,003-8,513,007 (genome assembly BDGP release 6) containing CG6745, the *PUS7 Drosophila* orthologue. Behavioral tests were performed on five-day-old flies with *Canton-S* as wild-type control. Wings were cut under cold anesthesia to one-third of their length on the evening before the experiment. Activity and orientation behavior was analyzed using Buridan's paradigm as described before.<sup>19</sup> All statistical groups were tested for normal distribution with the Shapiro-Wilk test. t-test analysis of variance with Bonferroni correction was used to compare different conditions. N=30 for all genotypes. Blinding was applied during the experiment. For the rescue experiment *pus7* cDNA was cloned downstream of a UAS promoter and the plasmid was injected into fly embryos. Positive recombinants were isolated based on eye color as the plasmid also carries the *white* gene.

### *Aggression assay*

A "handling free" behavior chamber described by Trannoy *et al.* (2015)<sup>20</sup> was used. Flies were constantly kept at 25°C. Male pupae were socially isolated. Aggression assay was applied on 6-day-old pairs of flies for 20 minutes. As food source apple juice agar with a drop of yeast was used. One day before analysis, flies were painted with acrylic ink during CO<sub>2</sub> anesthesia, since cold anesthesia leads to a decrease of aggressive behavior. Aggressive interactions including lunging, tussling, wing threat, boxing and chasing were evaluated for fights between wild-type *Canton-S* and homozygous *pus7<sup>fs</sup>* flies. In addition, the fighting index (averaged total time spend fighting) and the winner status were scored. The winner of a fight keeps pushing the opponent from the food source, whereas the loser retreats.

## Supplemental References

1. Abou Jamra, R., Wohlfart, S., Zweier, M., Uebe, S., Priebe, L., Ekici, A., Giesebrecht, S., Abboud, A., Al Khateeb, M.A., Fakher, M., et al. (2011). Homozygosity mapping in 64 Syrian consanguineous families with non-specific intellectual disability reveals 11 novel loci and high heterogeneity. *Eur J Hum Genet* 19, 1161-1166.
2. Reuter, M.S., Tawamie, H., Buchert, R., Hosny Gebiril, O., Froukh, T., Thiel, C., Uebe, S., Ekici, A.B., Krumbiegel, M., Zweier, C., et al. (2017). Diagnostic Yield and Novel Candidate Genes by Exome Sequencing in 152 Consanguineous Families With Neurodevelopmental Disorders. *JAMA Psychiatry* 74, 293-299.
3. Grimberg, J., Nawoschik, S., Belluscio, L., McKee, R., Turck, A., and Eisenberg, A. (1989). A simple and efficient non-organic procedure for the isolation of genomic DNA from blood. *Nucleic Acids Res* 17, 8390.
4. Riazuddin, S., Hussain, M., Razzaq, A., Iqbal, Z., Shahzad, M., Polla, D.L., Song, Y., van Beusekom, E., Khan, A.A., Tomas-Roca, L., et al. (2017). Exome sequencing of Pakistani consanguineous families identifies 30 novel candidate genes for recessive intellectual disability. *Molecular psychiatry* 22:1604-1614.
5. Amarasinghe, K.C., Li, J., and Halgamuge, S.K. (2013). CoNVEX: copy number variation estimation in exome sequencing data using HMM. *BMC Bioinformatics* 14 Suppl 2, S2.
6. Krumm, N., Sudmant, P.H., Ko, A., O'Roak, B.J., Malig, M., Coe, B.P., Project, N.E.S., Quinlan, A.R., Nickerson, D.A., and Eichler, E.E. (2012). Copy number variation detection and genotyping from exome sequence data. *Genome Res* 22, 1525-1532.
7. Pfundt, R., Del Rosario, M., Vissers, L., Kwint, M.P., Janssen, I.M., de Leeuw, N., Yntema, H.G., Nelen, M.R., Lugtenberg, D., Kamsteeg, E.J., et al. (2017). Detection of clinically relevant copy-number variants by exome sequencing in a large cohort of genetic disorders. *Genet Med* 19, 667-675.
8. Tawamie, H., Martjanov, I., Wohlfahrt, N., Buchert, R., Mengus, G., Uebe, S., Janiri, L., Hirsch, F.W., Schumacher, J., Ferrazzi, F., et al. (2017). Hypomorphic Pathogenic Variants in TAF13 Are Associated with Autosomal-Recessive Intellectual Disability and Microcephaly. *Am J Hum Genet* 100, 555-561.
9. de Ligt, J., Willemsen, M.H., van Bon, B.W., Kleefstra, T., Yntema, H.G., Kroes, T., Vulto-van Silfhout, A.T., Koolen, D.A., de Vries, P., Gilissen, C., et al. (2012). Diagnostic exome sequencing in persons with severe intellectual disability. *The New England journal of medicine* 367, 1921-1929.
10. Kumps, C., Van Roy, N., Heyrman, L., Goossens, D., Del-Favero, J., Noguera, R., Vandesompele, J., Speleman, F., and De Preter, K. (2010). Multiplex Amplicon Quantification (MAQ), a fast and efficient method for the simultaneous detection of copy number alterations in neuroblastoma. *BMC Genomics* 11, 298.
11. Wortmann, S.B., Vaz, F.M., Gardeitchik, T., Vissers, L.E., Renkema, G.H., Schuurs-Hoeijmakers, J.H., Kulik, W., Lammens, M., Christin, C., Kluijtmans, L.A., et al. (2012). Mutations in the phospholipid remodeling gene SERAC1 impair mitochondrial function and intracellular cholesterol trafficking and cause dystonia and deafness. *Nat Genet* 44, 797-802.
12. Vulto-van Silfhout, A.T., Nakagawa, T., Bahi-Buisson, N., Haas, S.A., Hu, H., Bienek, M., Vissers, L.E., Gilissen, C., Tzschach, A., Busche, A., et al. (2015). Variants in CUL4B are associated with cerebral malformations. *Human mutation* 36, 106-117.
13. Laemmli, U.K. (1970). Cleavage of structural proteins during the assembly of the head of bacteriophage T4. *Nature* 227, 680-685.
14. Schwartz, S., Bernstein, D.A., Mumbach, M.R., Jovanovic, M., Herbst, R.H., Engreitz, J.M., Guttman, M., Satija, R., Lander, E.S., Fink, G., et al. (2014). Transcriptome-wide Mapping Reveals Widespread Dynamic-Regulated Pseudouridylation of ncRNA and mRNA. *Cell* 159,148-162.



15. Dobin, A., Davis, C.A., Schlesinger, F., Drenkow, J., Zaleski, C., Jha, S., Batut, P., Chaisson, M., and Gingeras, T.R. (2013). STAR: ultrafast universal RNA-seq aligner. *Bioinformatics* 29, 15-21.
16. Safra, M., Nir, R., Farouq, D., Vainberg Slutskin, I., and Schwartz, S. (2017). TRUB1 is the predominant pseudouridine synthase acting on mammalian mRNA via a predictable and conserved code. *Genome Res* 27, 393-406.
17. Zaganelli, S., Rebelo-Guiomar, P., Maundrell, K., Rozanska, A., Pierredon, S., Powell, C.A., Jourdain, A.A., Hulo, N., Lightowlers, R.N., Chrzanowska-Lightowlers, Z.M., et al. (2017). The Pseudouridine Synthase RPUSD4 Is an Essential Component of Mitochondrial RNA Granules. *J Biol Chem* 292, 4519-4532.
18. Lence, T., Akhtar, J., Bayer, M., Schmid, K., Spindler, L., Ho, C.H., Kreim, N., Andrade-Navarro, M.A., Poeck, B., Helm, M., et al. (2016). m(6)A modulates neuronal functions and sex determination in *Drosophila*. *Nature* 540, 242-247.
19. Strauss, R., Hanesch, U., Kinkelin, M., Wolf, R., and Heisenberg, M. (1992). No-bridge of *Drosophila melanogaster*: portrait of a structural brain mutant of the central complex. *J Neurogenet* 8, 125-155.
20. Trannoy, S., Chowdhury, B., and Kravitz, E.A. (2015). A New Approach that Eliminates Handling for Studying Aggression and the "Loser" Effect in *Drosophila melanogaster*. *J Vis Exp*, e53395.
21. Consortium, G.T. (2013). The Genotype-Tissue Expression (GTEx) project. *Nat Genet* 45, 580-585.
22. Zwarts, L., Versteven, M., and Callaerts, P. (2012). Genetics and neurobiology of aggression in *Drosophila*. *Fly (Austin)* 6, 35-48.
23. Dankert, H., Wang, L., Hoopfer, E.D., Anderson, D.J., and Perona, P. (2009). Automated monitoring and analysis of social behavior in *Drosophila*. *Nat Methods* 6, 297-303.
24. Chen, S., Lee, A.Y., Bowens, N.M., Huber, R., and Kravitz, E.A. (2002). Fighting fruit flies: a model system for the study of aggression. *Proceedings of the National Academy of Sciences of the United States of America* 99, 5664-5668.
25. Nilsen, S.P., Chan, Y.B., Huber, R., and Kravitz, E.A. (2004). Gender-selective patterns of aggressive behavior in *Drosophila melanogaster*. *Proceedings of the National Academy of Sciences of the United States of America* 101, 12342-12347.